Chapter 3
Smart Materials in Active Vibration Control

Every feedback control system has essential components like the hardware computing control input via the strategy of our choice, sensors to provide feedback to this controller and actuators to carry out the required changes in plant dynamics. This chapter is concerned with the latter two components, that is sensors and actuators. More specifically, here we take a closer look at some of the advanced engineering materials that can be used as actuators and in some cases as sensors in active vibration control applications (AVC).

There are many well-known traditional actuating components such as electromagnetic devices, pneumatic actuators, rotary and linear motors etc., which may be effectively utilized in vibration control as well. Unlike the previously mentioned devices, modern engineering materials which are often referred to as *intelligent* or *smart* have the advantage of being lightweight and more importantly they can be seamlessly structurally integrated. For example, a composite aeroelastic wing equipped with thin piezoelectric wafers cast directly into the structure enables us to suppress undesirable vibration without adding a considerable mass or changing the shape of the wing. On the other hand, advanced materials like the magnetorheological fluid may add unprecedented properties to already existing components, for example creating automotive dampers with automatically adjusted damping properties. Figure 3.1 illustrates[1] an experimental actuator capable of providing displacements exceeding the usual range of simple piezoelectric materials [80]. The robust and low-cost high displacement actuator (HDA) made of pre-stressed polymeric materials and piezoelectric ceramics is an excellent example of advanced engineering smart materials. The aim of this chapter is to introduce the reader to some of these cutting-edge materials and their use in vibration control. Actuators like the aforementioned electromagnetic linear motors, pneumatic devices and others will not be covered here.

Thanks to the reciprocal physical effects experienced in some of these materials, actuating elements can also be used in a sensor configuration. Just as in the case of actuators, many feedback sensing systems exist other than the ones using smart

[1] Courtesy of NASA.

G. Takács and B. Rohal'-Ilkiv, *Model Predictive Vibration Control*,
DOI: 10.1007/978-1-4471-2333-0_3, © Springer-Verlag London Limited 2012

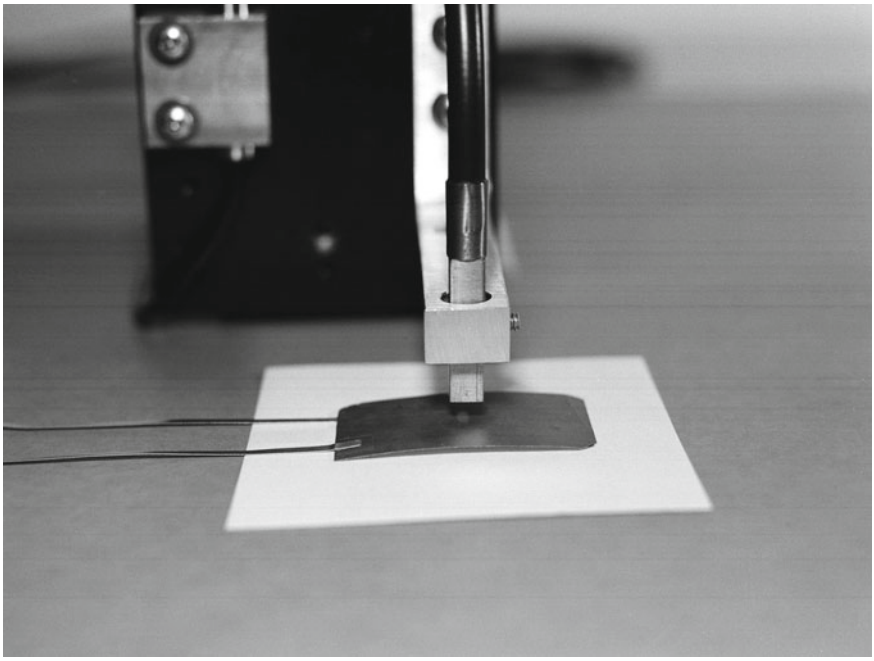

Fig. 3.1 An experimental high displacement actuator (HDA) developed at NASA Langley Research Center [80] is placed under a fiber optic displacement sensor

materials. Some of these are among others accelerometers,[2] strain sensors based on resistance wires, or more advanced devices like industrial laser triangulation heads or laser Doppler vibrometers (LDV). This chapter will concentrate on the materials themselves and the underlying physical aspects of the sensors in vibration attenuation, while introducing other possible feedback methods in a practical example in Sects. 5.3.4 and 5.5.3.

There are several engineering materials available nowadays, which exhibit some very desirable properties for use in AVC. So what is the criterion of classifying a material to be *smart?* The keyword here is coupling. From the structural point of view, the behavior of classical materials can be sufficiently described by their elastic constants: the elastic constant relates stress and strain, the thermal constant relates temperature and strain. In smart materials, coupling also exists between the either two (or even more) of the following fields: electric charge, strain, magnetic, temperature, chemical and light. This coupling is also obvious between the constitutive equations describing the behavior of these materials. The most common smart materials which are used in active structures are shape memory alloys, magneto- and electrostrictive materials, semi-smart magneto- and electro-rheological fluids where the coupling is one directional, electrochemical materials and of course piezoelectrics.

[2] However, these are also based on the piezoelectric effect and use piezoelectric materials [46].

The chapter begins with a discussion on the shape memory effect and shape memory alloy materials. In addition to the shape memory effect, the passive albeit still very interesting superelastic nature of these materials is also introduced. After characterizing the interactions between the applied temperature, stress and strain; the utilization of shape memory alloys in vibration control is reviewed. Section 3.2 addresses the magnetostrictive and electrostrictive effect and their use in vibration attenuation. Following this, the popular magnetorhoeologic fluids and the related electrorheological fluids are introduced, also with a short review of their existing and potential applications in active vibration control. The next section, that is 3.4, deals with the piezoelectric effect and piezoelectric materials. In addition to the physical basis, some of the mathematical modeling concepts and finite element analysis aspects are also covered. Our selection of smart materials ends with a section on the emerging electrochemical polymer based actuators in Sect. 3.5. A couple of short paragraphs on other types of materials and actuators end our discussion on smart materials in AVC.

3.1 Shape Memory Alloys

Shape memory alloys (SMA) demonstrate apparent plastic deformation and recovery to the original shape after heating. SMA can recover as much as 5% strain, which compared to materials like piezoceramics is a considerable shape change. The main advantage of this type of smart material is the ability to perform complex movements with few elements. The shape change and the resulting movement can be achieved by a small temperature change, and causes the SMA to undergo a type of solid state phase transformation. This change is the so-called martensitic deformation in metals. Shape memory alloys may be used to supply energy to systems with very slow dynamics and thus induce vibrations, effectively creating an active vibration control system. It is also common to utilize the SMA as a type of slowly changing adaptive part to form a semi-active vibration suppression system [33]. Figure 3.2 illustrates[3] the use of shape memory alloy materials to create slow-speed morphing wing surfaces on aircraft and SMA-wire based linear motors.

3.1.1 SMA Materials and Properties

The most common SMA material is an alloy of nickel and titanium, which is often referred to as nitinol.[4] In the nickel and titanium (NiTi)-based alloys, the two elements are present in approximately equal atomic percentages. Several other alloys exist of which we list FeMnSi, copper-based alloys such as CuZnAl or CuAlNi and some

[3] Courtesy of NASA.

[4] This nickel and titanium alloy was discovered and developed by Buechler et al. in 1963 at the U.S. Naval Ordnance Laboratory, thus the name NiTiNOL.

(a) A wing-like SMA demonstration device **(b)** SMA based actuators

Fig. 3.2 A SMA-based demonstration device resembling an aircraft surface is featured in (**a**) [78], while (**b**) shows small actuators in a linear motor mode based on SMA wires [79]

steel formulations [28, 33]. The advantage of NiTi-based SMA is its high electric resistivity, thus allowing the material to be rapidly heated upon the application of electric current.

Shape memory alloys present two interesting macroscopic properties, these are:

- superelasticity
- shape memory effect

The former, superelasticity is the ability of this type of material to return to its original shape after a considerable amount of mechanical stress and deformation. This process needs no temperature change to be completed, and it is called the mechanical memory effect. Elasticity is approximately 20 times higher than other elastic metallic materials [68]. Objects manufactured from the superelastic version of nitinol find their application mainly as medical instruments, there are several laboratory experiments investigating the use of superelastic (austenitic) nitinol as means for passive vibration damping.

The latter property is more interesting for the control community, as nitinol can be effectively used as an actuator. Because of the shape memory effect or the thermal memory effect, the plastically deformed SMA material returns to its original memorized shape after applying a small amount of heat as illustrated in Fig. 3.3. The deformation is not limited to pure bending as in bi-metallic structures, but may include tensional and torsional deformations or their mixtures [68]. A 4 mm diameter nitinol wire may lift even a 1000 kg load; however, it will lose its memory effect because of this large loading. To prevent this, a load limit is usually enforced, for example, in this case a 150 kg load would not induce a loss of the memory effect while still being a very high force output [68]. Enforcing such load limits to prevent the loss of the memory effect call for control systems encompassing constraint handling for which model predictive control (MPC) is an ideal candidate.

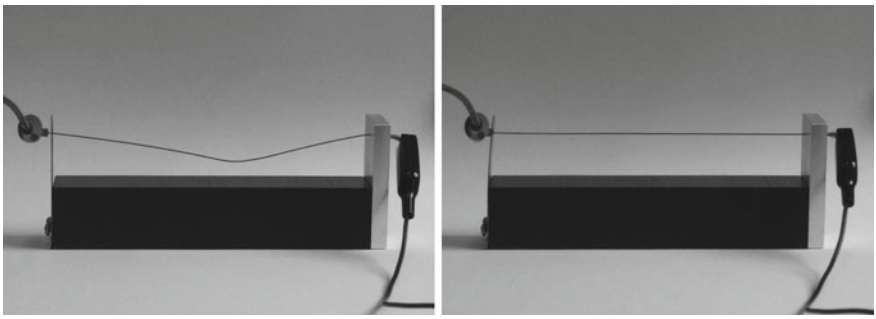

(a) SMA wire prior to activation **(b)** SMA wire after activation

Fig. 3.3 An SMA wire is placed in between a spring steel blade and a rigid aluminum clamp. The wire is loose prior to activation as shown in (**a**). Due to the applied current (9 V battery) the wire temperature is raised above the activation temperature. The wire regains its original straight shape in (**b**) and exerts a force, which is enough to deform the spring steel

3.1.2 Stress, Strain and Temperature

Both the superelastic and shape memory effects are due to a phase change from *austenite*, which is the higher temperature and stronger phase, to *martensite* which is the lower temperature and softer phase. Unlike the phase changes that come to mind like the change from solid to liquid and gas, this is a solid phase change. The austenitic solid phase is stable at elevated temperatures and has a strong body centered cubic crystal structure. The martensitic phase has a weaker asymmetric parallelogram structure, having up to 24 crystal structure variations [101]. When martensitic nitinol is subject to external stress it goes through different variations of the possible crystal structures and eventually settles at the one allowing for maximal deformation. This mechanism is called *detwinning*. There are four temperatures characterizing the shape memory effect of SMA:

- M_f: martensite finish—this is the lowest temperature, below all of the material has the soft martensitic structure
- M_s: martensite start—an intermediate temperature, when the martensite phase starts to appear in the prevalently austenitic phase
- A_s: austenite start—an intermediate temperature, when the austenite phase starts to appear in the prevalently martensitic phase
- A_f: austenite finish—this is the highest temperature, above which all of the material has the hard martensitic structure. Superelastic SMA are designed to work over this temperature, while the thermal-induced memory effect finishes at this temperature

These temperature characteristics and limits may be set upon manufacturing the alloy. For example, it is possible to create an alloy with a reshaping temperature close to the normal temperature of the human body.

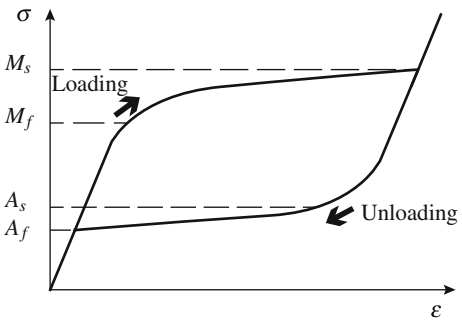

Fig. 3.4 Pseudoelastic behavior of shape memory alloys, illustrated on a stress-strain hysteresis curve

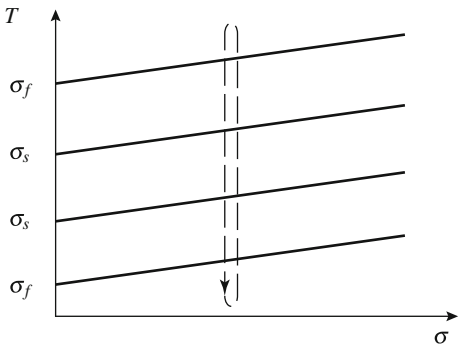

Fig. 3.5 Thermal memory effect of SMA in relation to constant stress and variable temperature

For the case of uniaxial loading, the stress–strain curve for SMA is denoted in Fig. 3.4 [99]. The curve shows a pseudoelastic behavior, where the applied load takes the material from the austenite phase to the martensite phase along the upper curve. This is the stress-induced superelastic behavior of austenitic nitinol, therefore we may state that the temperature here is a constant $T > A_f$. The reverse transformation occurs in unloading the SMA material, when the material transforms from martensite into austenite along the lower curve, thus forming a hysteresis loop [99]. In Fig. 3.4 ε denotes strain, σ denotes stress. Martensite starts to form at M_s and finishes at M_f, while the austenite starts to form at A_s and finishes at A_f.

The dashed line in Fig. 3.5 denotes a scenario, where the SMA is subject to a temperature change in constant stress [99]. Note, however that the phase change start and finishing temperatures are linearly dependent on the loading stress. Temperature is marked by T while stress is σ.

Finally, Fig. 3.6 illustrates the percentual composition of martensite and austenite phases in a temperature-induced martensitic deformation [101]. The curve starts from below the low temperature M_f and takes the right side of the hysteresis path. At a certain A_s temperature the phase change to austenite begins, while the martensite composition decreases. Eventually the material gets to the A_f temperature where 100% of it is converted into the austenite phase.

Shape setting of an SMA actuator can be done in a high temperature oven. The heat treatment is performed in two steps: first the material is constrained into the desired

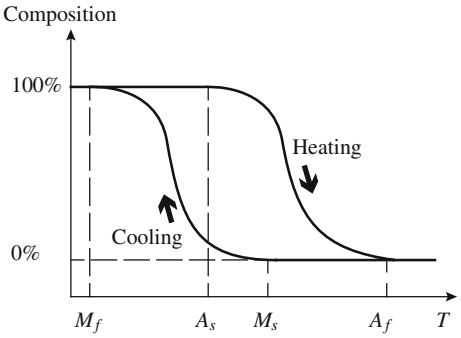

Fig. 3.6 Temperature dependent deformation: austenitic-martensitic phase transformation hysteresis of shape memory alloys

form, and heated at 525°C for 5–10 min depending on the size of the clamp. After this, the material is quenched with air cooling, water or oil. This is then followed by a repeated heating at 475°C for about 30–60 min [69]. Figure 3.7 illustrates SMA materials memorized to different shapes. While the plates on the left and the wire is memorized to a flat (straight) shape, the third and darker plate is memorized into a curved shape.

3.1.3 SMA in Vibration Control

The free and/or forced vibration behavior of plates and other structures with embedded SMA materials is studied using analytic or FEM methods in [35, 54, 99, 85, 130]. The cited works focus on modeling issues for the need of optimal design for classical vibration response manipulation, without actively controlled components. The inclusion of SMA elements in plates, beams and other mechanisms can be understood as a form of semi-active control. SMA has been already considered as passive or semi-active vibration damping devices in civil engineering structures [43, 126, 101].

Although several models have been proposed for SMA, the constitutive description of the complex pseudoelastic and shape memory effect phenomena cannot be developed by classical plasticity theory. Models based on the nonlinear generalized plasticity have been successfully applied for SMA [28].

SMA as an actuator is suitable for low frequency and low precision applications, therefore, their usage in active vibration attenuation applications is questionable. It is interesting enough to note that SMA can also be used as a type of sensor. The work of Fuller et al. pointed out that embedded SMA wires in a Wheatstone configuration may give accurate estimation of strain levels due to oscillations in a beam [33]. The use of SMA as sensors is, however, atypical as piezoelectric or resistance-wire based sensors are also cheap and readily available.

Active vibration control is proposed utilizing an SMA actuator in [22]. Here, the temperature of the SMA is manipulated to change mechanical properties.

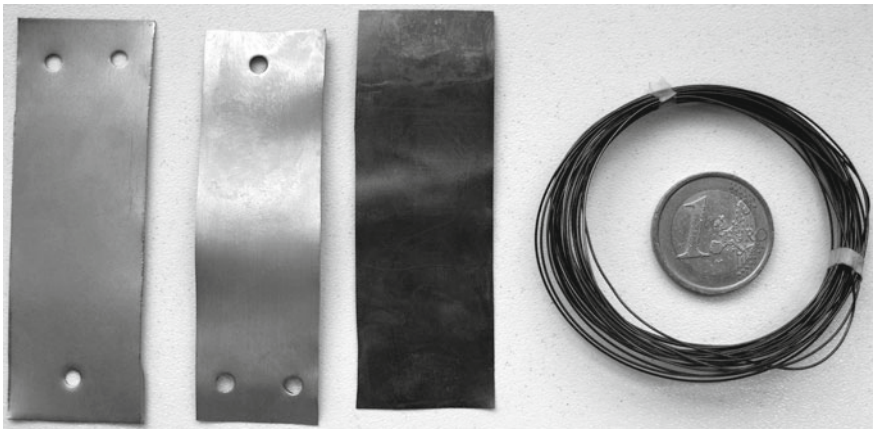

Fig. 3.7 SMA materials can be memorized to different shapes. The wire and the plates on the *left* are set to a straight shape, while the darker plate is memorized to a curved shape

Vibration damping is achieved combining active and passive methods. In a review article Bars et al. lists shape memory alloys as a particularly interesting tool for smart structures and states the need for advanced control algorithms such as MPC to tackle issues such as multi-point inputs and outputs, delays and possibly actuator nonlinearity [13].

Shape memory alloy materials are utilized in [23] for vibration damping purposes. According to the step response of the material, upon the application of a constant current jump the SMA wire exerts force, which can be approximated according to a first order response [15, 23]:

$$T_c \frac{df(t)}{dt} + f(t) = i(t) \tag{3.1}$$

where the force exerted by the SMA wire is denoted by $f(t)$, the actuating current by $i(t)$ while T_c is the time constant of the first order transfer. The temperature in an SMA wire actuator is approximately linearly dependent on the applied current [54]. Unfortunately, the time constant is different in the heating and cooling cycles [23, 24]. The time constant is also highly dependent on the prestrain applied to the wire. Because of these parameter variations it is likely that an MPC control-based SMA system would require the explicit handling of model uncertainties. The above cited work of Choi et al. utilized sliding mode controlled nitinol wires to damp the first modal frequency of a building-like structure in the vicinity of 5 Hz, providing certain basis to use SMA for lightly damped structures with a low first resonant frequency. Here, the time constant was approximated to be 125 ms that would indicate an approximately 8 Hz bandwidth.

A very interesting possibility is utilizing an adaptive passive approach instead of actively controlling the vibration amplitudes, velocities or accelerations. Using a structure or mechanism with integrated SMA parts, one could tune its vibration

(a) SMA wire **(b)** SMA actuated F-15 inlet

Fig. 3.8 Spools of shape memory alloy wires with different diameters are shown in (**a**), while (**b**) shows a full-scale F-15 inlet (modified flight hardware) with integrated shape memory alloy actuators installed in the NASA Langley Research Center 16-foot Transonic Tunnel [81]

frequency in real-time according to the outside excitation [33]. By this method, the resonant frequency of the structure could actively adapt to the quality and character of the measured outside excitation. Using the idea an actively controlled steel structure has been presented in [86]. The resonant frequency of the structure could be shifted about 32% of its nominal value through the application of heat into the SMA.

An overview of the civil engineering applications of SMA materials is given in [47]. John and Hariri investigate the effect of shape memory alloy actuation on the dynamic response of a composite polymer plate in [49]. The work examines the stiffness change and thus the shift of natural frequencies in a composite plate both in simulation and in experiment, founding a basis for the future application of SMA-enhanced active materials for vibration attenuation. Spools of SMA wire with different diameters are illustrated in Fig. 3.8a, while an SMA actuated F-15 aircraft inlet is shown[5] in Fig. 3.8b.

3.2 Magneto- and Electrostrictive Materials

Both magnetostrictive and electrostrictive materials demonstrate a shape change upon the application of magnetic or electric fields. This small shape change is believed to be caused by the alignment of magnetic/electric domains within the material upon the application of the fields. The advent of specialized engineering materials enables the use of these materials in active vibration control applications thanks to the increased deformation strains.

[5] Courtesy of NASA.

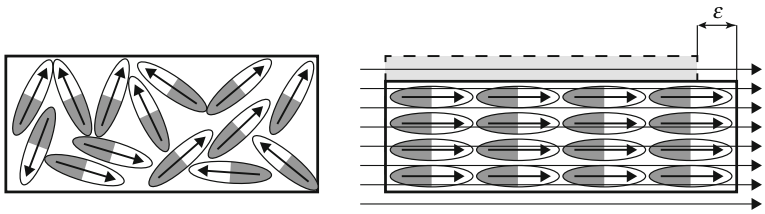

Fig. 3.9 Inactive magnetostrictive material with randomly ordered dipoles is shown on the *left*, while the *right* side shows an activated magnetostrictive material under a magnetic field. The dipoles have been ordered along the magnetic flux lines causing the material to expand

3.2.1 Magnetostrictive Materials

Magnetostrictive (MS) materials change their shape when subjected to a magnetic field. A common example of the magnetostrictive effect in everyday life is the humming noise emitted by electric transformers. This is due to the expansion and contraction of metallic parts in response to magnetostriction, induced by the changing electromagnetic field. Nearly all ferromagnetic materials demonstrate this property, but the shape and volume change is very small. Ferromagnetic materials have a structure divided into magnetic domains exhibiting uniform magnetic polarization. The applied magnetic field causes the rotation of these domains and in return a slight shape change on a macroscopic level. Figure 3.9 illustrates the randomly oriented magnetic domains within the material and the reorientation after the magnetic field is applied. The reciprocal phenomenon to magnetostriction is called the *Villari effect*. This describes the change of magnetic properties under applied load.

The deformation in magnetostrictive materials is characterized with the magnetostrictive coefficient ι_{ms}, which expresses the fractional length change upon applying a magnetic field. The shape change of the material is zero at zero magnetic field, however upon the application of the field it grows linearly according to the magnetostrictive coefficient until the material reaches magnetostrictive saturation.

The application of certain rare earth materials into an alloy allowed using the effect of magnetostriction in real-life engineering applications. Early types of magnetostrictive alloys demonstrated large magnetostriction, but only by applying high magnetic fields or at cryogenic temperatures [51]. These difficulties were eliminated by the introduction of *Terfenol-D*,[6] which continues to be the most common magnetostrictive material [1]. Terfenol-D exhibits about 2000 $\mu\varepsilon$ at room temperature, while Cobalt, which demonstrates the largest magnetostrictive effect of the pure elements, exhibits only 60 $\mu\varepsilon$ strain. Another common material goes by the trade name *Metglas 2605SC*, yet another by *Galfenol*.

[6] Similar to nitinol, it has been invented at the United States Naval Ordnance Laboratory (NOL). Terfenol-D stands for Terbium Ferrum NOL Dysprosium; with the chemical composition $Tb_x Dy_{1-x} Fe_2$.

The typical recoverable strain of magnetostrictive materials like Terfenol-D is in the order of 0.15%. Maximal response is presented under compressive loads. Magnetostrictive actuators have a long life span and may be used in high precision applications. Actuators may be used in compression alone as load carrying elements. Pre-stressing the actuators may increase both efficiency and the coupling effects [18].

3.2.2 Electrostrictive Materials

Electrostriction is closely related to magnetostriction. Due to electrostriction, all dielectrics change their shape upon the application of an electric field. The physical effect is similar to magnetostriction as well: non-conducting materials have randomly aligned polarized electrical domains. If the material is subjected to a strong electric field, the opposing sides of these domains become charged with a different polarity. The domains will be attracted to each other, thus reducing material thickness in the direction of the applied field and elongating it in a perpendicular direction.

All dielectrics exhibit some level of electrostriction; however, a class of engineering ceramics does produce higher strains than other materials. Such materials are known as *relaxor ferroelectrics* [56, 116] for example: lead magnesium niobate (PMN), lead magnesium niobate-lead titanate (PMN-PT) and lead lanthanum zirconate titanate (PLZT).

The elongation of electrostrictive materials is related quadratically [117] to the applied electric field [116]:

$$\varepsilon = \text{const} \cdot E^2 \tag{3.2}$$

where ε is strain and E is electric field strength. The relative percentual elongation for PMN-PT is 0.1% or 1000 $\mu\varepsilon$, but this is achieved under a field strength of 2 MV/m. Typical strains for special electrostrictors is in the range of 0.02−0.08%.

3.2.3 Magneto- and Electrostrictive Materials in Vibration Control

A mechanically amplified MS actuator for low frequency (1-10 Hz) vibration damping applications is suggested in [14], where the achievable displacement is rated between 0.5–4 mm and the force between 0.5–6 kN. Commercial actuator prototypes are also available; examples of such actuators are featured in Fig. 3.10[7] [20].

From the point of vibration control, MS actuators may deliver a high force output with high frequency [18, 73]. The underlying dynamics is a complex combination of electrical, mechanical and magnetic phenomena, which is further complicated by

[7] Courtesy of the CEDRAT Group.

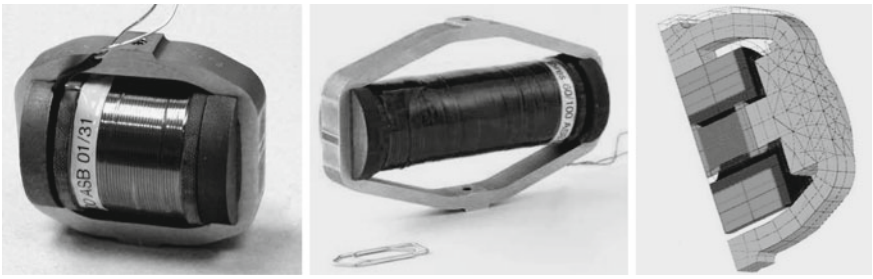

(a) Miniature MS actuator **(b)** MS actuator **(c)** FEM analysis

Fig. 3.10 Prototypes of different magnetostrictive actuators are shown in (**a**) and (**b**), while (**c**) features a FEM simulation of a deformed magnetostrictive actuator [20]

the nonlinear hysteretic behavior of Terfenol-D [18]. The linear properties of MS actuators hold only under the following assumptions [18]:

- low driving frequency
- reversible magnetostriction without power loss
- uniform stress and strain distribution

Under these assumptions the magnetomechanical equations are [27]:

$$\mathbf{S} = \mathbf{s}_H \sigma + \mathbf{g}\mathbf{H}_\mathbf{m} \tag{3.3}$$

$$\mathbf{B}_\mathbf{m} = \mathbf{g}\sigma + \mu_\sigma \mathbf{H}_\mathbf{m} \tag{3.4}$$

where $\mathbf{S}$ is strain, σ is stress, $\mathbf{s}_H$ is mechanical compliance at constant applied magnetic field strength $\mathbf{H}$, $\mathbf{g}$ is the magnetic cross-coupling coefficient, μ_σ is magnetic permeability at constant stress and $\mathbf{B}_\mathbf{m}$ is magnetic flux within the material.

Piezoelectricity is in fact a subclass of electrostrictive materials. However, while electrostrictive materials are nonlinear, piezoelectric materials behave linearly, which is an important feature for control applications. Moreover, electrostriction is not a reversible effect; unlike magnetostriction or piezoelectricity, the material does not generate an electric field upon the application of a mechanical deformation. Another important feature of electrostrictive materials is that they do not reverse the direction of the elongation with a reversed electric field [109]—note the quadratic dependence in (3.2). Therefore, electrostrictive transducers must operate under a biased DC electric field [116]. In comparison with piezoelectric materials, electrostrictive materials demonstrate a smaller hysteresis [109].

Braghin et al. introduces a model of magnetostrictive actuators for active vibration control in [18]. The authors propose a linear model for MS actuators, which is suitable for control design below the 2 kHz frequency range. This simple linearized numerical model has provided a good match with the experimental result for an inertial type of MS actuator. Such a linearization is not only important for the design of traditional feedback control systems, but is also essential for real-time model predictive control

using MS actuators. Despite the complicated coupling, hysteresis and nonlinearity the static actuation displacement of MS actuators remains linear [73]. A linear SDOF system is the basis for the further analysis of the behavior of an MS actuator in a work by Li et al. as well [58].

The vibration suppression of composite shells using magnetostrictive layers is discussed in a work by Pradhan et al. [90]. The author formulated a theoretical model for composite shells and found that magnetostrictive layers should be placed further away from the neutral plane. In addition, thinner MS layers produced better damping. The MS actuator-based vibration damping of a simply supported beam is discussed by Moon et al. [73], where the experimental setup shows a significant reduction of vibrations in comparison with the scenario without control.

The use of electrostrictive actuation in vibration control is relatively uncommon. Sonar projectors are the typical field of use for electrostrictive actuators [89]; however, this does not concern vibration attenuation rather generating acoustic waves. An electrostrictive actuator has been utilized by Tzou et al. in [117] for the control of cantilever vibrations. Tzou et al. achieved only minimal damping under control when compared to the free response without actuation.

3.3 Magneto- and Electrorheological Fluids

Fluids based on the magnetorheological (MR) and electrorheological (ER) effects contain suspended particles, which upon the application of a magnetic/electric field align themselves to form columns within the fluid. The columns of suspended particles create an obstacle for fluid flow, thus increasing the overall net viscosity of the system. Damping systems using MR or ER fluids cannot supply energy to the controlled system, but may change the damping properties according to a controller strategy.

3.3.1 Magnetorheological Fluids

Magnetorheological fluids (MR) contain micrometer-sized particles in a dielectric carrier fluid [105]. The carrier fluid is usually a type of oil, while the particles are manufactured from multi-domain, magnetically soft materials such as metals and alloys [5]. MR fluids respond to an applied magnetic field. Upon application of a magnetic field, the MR fluid changes viscosity up to the point where it can be considered as a viscoelastic solid. It is worth noting that this behavior can be regarded as semi-active. This is because it is needed to use an external field to induce classical coupling. There is also the lack of reciprocal effect. The controlled system will remain conservative from the mechanical point of view and can only dissipate energy [92].

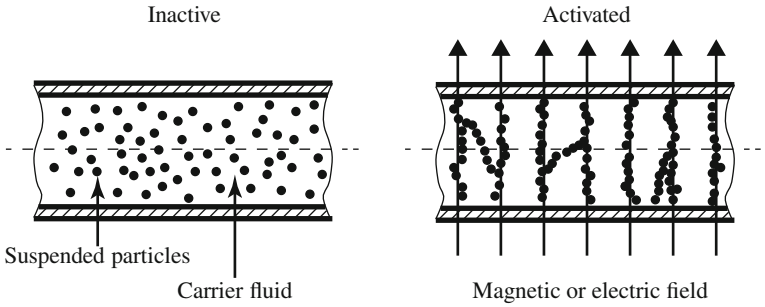

Fig. 3.11 Inactive MR fluid with suspended particles without an applied magnetic field is shown on the *left*, while the particles aligned to columns according to magnetic flux lines are featured on the *right*. ER fluids behave very similarly, but the material is activated by a strong electric field

Magnetorheological fluids are different from ferrofluids mainly in the size of the suspended particles. Brownian motion keeps the nanometer-sized particles constantly suspended in ferrofluids. The micrometer-sized particles in MR fluids are not subject to this phenomenon, therefore they eventually settle in the fluid because of the density difference of the carrier and the particles.

A typical magnetorheological fluid contains 20–40% by volume, 3–10 μm diameter iron particles [61]. These particles are suspended in a carrier liquid which can be mineral oil, synthetic oil or even water and may contain proprietary additives [5]. Additives prevent the suspended particles from settling due to the gravitational effect, decrease wear and modify viscosity.

When a magnetic field is applied to such a two-phased suspension, the randomly placed particles align themselves along the flux lines as illustrated in Fig. 3.11. In this way the flow of liquid is restricted in a direction perpendicular to the magnetic flux. The yield stress of magnetorheological fluids is typically 20–50 times higher than electrorheological fluids [91]. MR fluids are temperature stable, need low power supply and are able to react in a fully reversible fashion within milliseconds. The type of the aligned particle chains may vary if the MR liquid is activated in microgravity, ultimately changing its viscosity properties. Figure 3.12[8] shows the particles aligned to spikes in Earth gravity on the left, while the particle columns are broader in space.

3.3.2 Electrorheological Fluids

Electrorheological fluids (ER) differ from magnetorheological in the form of control coupling: while MR is controlled indirectly through the application of a magnetic field, ER is controlled through a direct electric field [105]. ER fluids contain

[8] Courtesy of NASA.

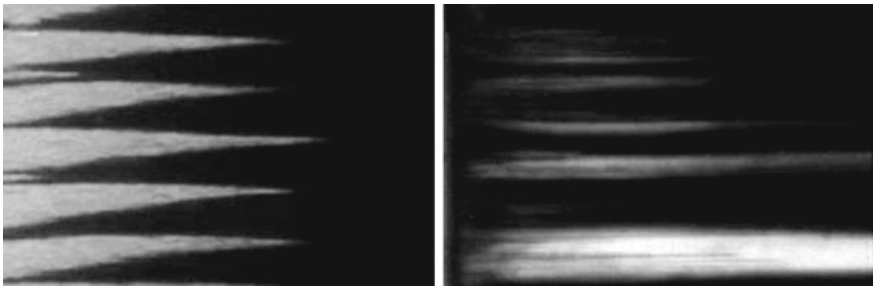

(a) Earth gravity **(b)** Microgravity

Fig. 3.12 Video microscope images of magnetorheological (MR) fluids. The MR fluid forms columns or spiked structures on Earth, while on the *right* broader columns are formed in microgravity environment aboard the International Space Station (ISS) [82]

non-conducting particles up to 50 μm in diameter and similar to MR fluids have a reaction time measurable in milliseconds. When we describe the consistency of the activated MR material from a practical point of view, we may refer to it as a kind of viscoelastic solid while the activated ER fluid resembles the consistency of a gel-like substance. In addition to the composition of the ER fluid, its behavior is greatly dependent on the geometry such as the size and distance of the plates acting as electrodes. This is similar to the design of capacitors, where capacitance in addition to the type of dielectric material used is influenced by electrode spacing and geometry.

The behavior of electrorheological fluids can be described by two alternative theories [104]: electrostatic theory and the interfacial tension theory. Electrostatic theory assumes a behavior similar to the MR fluids: the particles align in accordance to the electrical field to form chain-like structures. According to the interfacial tension theory, the ER liquid consists of three phases: the suspension liquid, the particles and another liquid within the particles. In the inactive state, this liquid is contained within the dispersed particles. When the liquid is activated, the electric field drives the liquid within the particles to a certain side through electroosmosis—and because of that neighboring particles start to bind and formulate chains on a macroscopic level. While no conclusion has been reached, it is possible that different types of ER materials exist which behave according to different principles.

3.3.3 Magneto- and Electrorheological Materials in Vibration Control

There are three possible operation modes for MR and ER fluid based semi-active damping devices. These modes are [105]:

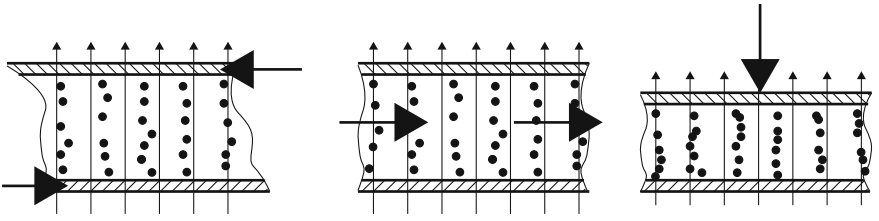

Fig. 3.13 Different operation modes for an MR fluid-based damping device. The figure shows shear, flow and squeeze modes (from *left* to *right*). Thick arrows denote movement directions, while thin arrows represent magnetic flux lines

- shear
- flow
- squeeze

To get an idea of these different operation modes, let us imagine a situation when the MR fluid is placed between two parallel plates. The magnetic field is acting perpendicular to these plates; therefore, the particles align themselves perpendicularly as well. In shear mode, one plate is moving in relation with each the other in a direction perpendicular to the magnetic flux and the particle columns. In flow mode, the plates are stationary and the fluid is moving due to a pressure difference. In the squeeze-flow mode, the plates are moving in relation to each other, however this time the movement is carried out along the flux lines and the particle columns. Operation modes of different MR and ER fluid based devices are illustrated in Fig. 3.13. The vibration damping performance of flow and squeeze mode semi-active insulation mounts with ER fluid actuators is discussed by Hong and Choi in [41], concluding that the squeeze mode actuator is more effective than the flow mode.

Mathematically, it is somewhat difficult to represent the behavior of MR and ER materials. The reason for this is that the model must account for hysteresis and static friction. The yield stress of the fluid is also variable: in the presence of a magnetic (electric) field the MR (ER) fluid acts as a solid, up to the point where the shear stress is reached (yield point).

The most common mathematical description is the so-called Bingham plastic model, which utilizes variable yield strength τ_Y. This depends on the strength of the applied magnetic field H. There is a point where the increased magnetic field H does not have an effect on the yield, the MR fluid is magnetically saturated. The flow is governed by the equation [87]:

$$\tau = \tau_Y(H) + \eta_v \dot{\gamma_s} \tag{3.5}$$

where shear stress is expressed by τ, shear strain by γ_s and fluid viscosity by η_v. Below the yield stress, the material exhibits viscoelastic properties, which may be described by:

$$\tau = G\gamma_s \tag{3.6}$$

where G is the complex material modulus. The Bingham plastic model is a good approximation for the activated MR and ER fluids with the respective substitutions for τ_Y, η_v, γ_s. In reality, the dynamic behavior of MR and ER fluids differs from the Bingham plastic model, for example in the absence of magnetic field, because the fluid is slightly non-Newtonian and its behavior is temperature dependent.

The above-mentioned types of semi-smart materials also have a few drawbacks: namely that they demonstrate high density (weight), good quality fluids are expensive and are prone to sedimentation after prolonged use. Particle sedimentation is controlled by surfactants; recent studies also used nanowire particles to decrease the sedimentation effect [83]. Sedimentation in ER fluids is prevented by using particles of densities comparable to the density of the fluid phase. Another disadvantage is that both MR and ER fluids have low shear strength; this is in the range of 100 kPa for MR [5]. Shear strength in both MR and ER can be improved by fluid pressurization [71, 122] while it can be further increased in MR using elongated particles [120].

In addition to sedimentation and low shear–stress, ER dampers require a high potential electric field to operate which is in the order of 1 kV for an electrode separation and fluid thickness of 1 mm.

From the control point of view, the dynamic behavior of MR and ER dampers is highly nonlinear, creating a considerable difficulty when designing a control algorithm. Controllers such as positive position and velocity feedback, acceleration feedback based LQ control, have been successfully utilized to generate control voltage to MR dampers. The operating voltage in ER fluids is close to the breakdown voltage of the material, therefore a constrained controller such as MPC is highly recommended to prevent actuator failure and increase lifetime while maintaining maximum actuating efficiency.

Flow mode MR dampers are used to control linear vibrations. Rotational motion can be controlled by using a shear mode damper, while a squeeze flow setup mode is useful for vibration damping platforms. The relatively large size of MR dampers prevents their use in certain application fields, such as submarines [5]. The use of MR dampers in earthquake control is favored because of low power requirements and high reliability [128]. Magnetorheological dampers are often utilized for the vibration damping of vehicle suspensions and civil engineering structures [5, 57, 67, 121]. MR dampers have been also suggested for the semi-active damping of washing machine vibrations in [103].

In addition to experimental vibration damping applications [42, 50, 107], ER materials have been successfully utilized in clutches [72] and brakes, machine tool vibration control in [123], engine suspensions in [125] and others. They have been considered to use in haptic displays and to create bulletproof vests. An ER fluid based composite sandwich material is suggested in [62]. The authors investigated the modal properties of such a system under different electric loads and arrived at the conclusion that the resonant frequencies shift up and peaks decrease with an increasing field strength. Such a composite smart structure could be very interesting for the

aviation and space industry. Yet other applications for vibration control through MR-or ER-based dampers are featured in [17, 25, 134, 110].

3.4 Piezoelectric Materials

Piezoelectricity is the ability of certain materials to generate an electric charge in response to an applied stress. If the material is not short-circuited, the charge induces a voltage. This is the so-called *direct piezoelectric effect*. The piezoelectric effect is reversible, meaning that applied voltage generates mechanical stress and deformation. This is known as the *converse piezoelectric effect*. Piezoelectric materials are common in everyday appliances, such as sound reproduction instruments [96], igniters, optical assemblies and other devices. Due to the unique properties of piezoelectric materials, their application is also widespread in active vibration control and its related fields.

The usage of piezoelectric transducers as both sensors and actuators is demonstrated in Fig. 3.14[9] with the Aerostructures Test Wing (ATW) experimental device designed and used at NASA's Dryden Flight Research Center. The ATW is equipped with an array of piezoelectric patches, used in sensor mode to estimate aeroelastic flutter effects on the wing [77]. The wing is intentionally driven to mechanical failure, in order to assess flutter effect. This experiment is carried out by mounting the ATW to a testbed aircraft, but the larger piezoelectric patches are used as actuators to excite the structure to induce structural failure artificially. The figures and the experiment not only demonstrate the dual usage of piezoelectric transducers, but also point out the dramatic effects and real power of mechanical systems driven through piezoceramics.

3.4.1 The Piezoelectric Effect and Materials

A piezoelectric material mounted with electric terminals is illustrated in Fig. 3.15a where no strain change ($\varepsilon_{in} = 0$) is induced in the absence of deformation and no voltage ($V_{out} = 0$ V) can be measured on its terminals. Upon the application of deformation, the strain change induces charge within the material and a measurable voltage on the output. The piezoelectric material acts as a strain or deformation sensor. This direct piezoelectric effect is illustrated in Fig. 3.15b graphically. An initial situation identical to the previous case is illustrated in Fig. 3.15c, where no strain or voltage can be measured on the material and its terminals. Here however, the material works as actuator, taking advantage of the converse piezoelectric effect as illustrated in Fig. 3.15d. Upon the application of an input voltage to the terminals, a deformation thus a strain change is induced in the material. Note that the strain change $\varepsilon_{out} \neq 0$ is maintained only as long as there is an input voltage on the

[9] Courtesy of NASA.

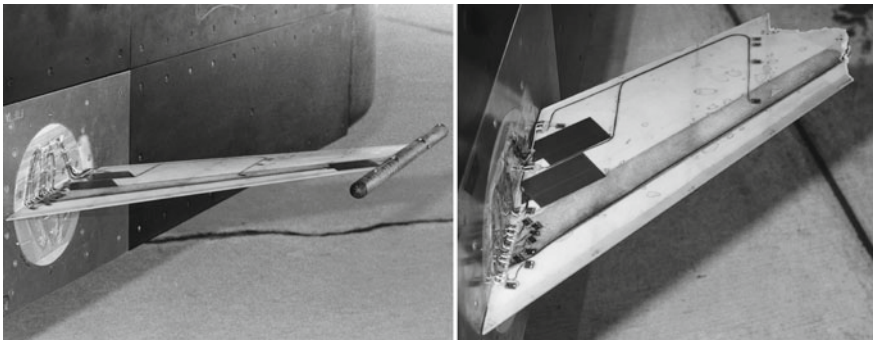

(a) Wing before failure **(b)** Wing after failure

Fig. 3.14 An aerostructures test wing (ATW) is pictured in (**a**), while the same device is shown in (**b**) after intentional failure. Piezoelectric transducers are mounted on the surface and visible on the image [75, 76]

terminals. Moreover, the strain change can be induced with DC voltage change as well. In the direct case, only dynamic strain changes are detected. In other words, steady-state deformations $\varepsilon_{out} \neq 0$ are not included in the output signal V_{out}, only the strain changes are represented.

The direct and converse piezoelectric effect is due to the electric (piezoelectric) domains or dipoles within the material [33]. In fact, the piezoelectric effect is a special case of the electrostrictive effect, where the randomly oriented electric domains in all dielectric materials orient themselves along the flux lines of an applied electric field, causing slight deformations. Although there are naturally occurring piezoelectric materials (quartz,topaz, Rochelle salt, cane sugar), today's applications use engineered polycrystalline materials such as lead-zirconate-titanate (PZT), lead titanate (PT), lead magnesium niobate-lead titanate (PMN-PT); more recently macrofiber composites (MFC) and ammonium dihydrogen phosphate (ADP); or the environmentally friendly lead-free ceramics such as bismuth sodium titanate (BNT), tungsten-bronze (TB), and others [26, 65, 94, 133]. PZT is probably the most commonly utilized piezoelectric material utilized in commercially available transducers. Piezoelectric transducers are relatively cheap to manufacture, and are available in an array of shapes and sizes. The material itself is hard and brittle. By the process of *poling* or *polarization*, the dominant geometry of the piezoelectric material can be set at the manufacturing stage. Both the direct and the converse piezoelectric effects will dominate this *polarization* direction.

The amount of deformation depends on the type of piezoelectric material in use. In addition to the material type, the size, geometry, positioning and the amount of applied voltage are also contributing factors in the achievable deformation. For PZT the percentual elongation is typically 0.1%. In addition to precision systems and nanopositioning, there are numerous examples where piezoelectric transducers can be used directly with or without mechanical amplification. For example [38] considers the use of PZT wafers in cyclic and collective pitch control of UAV

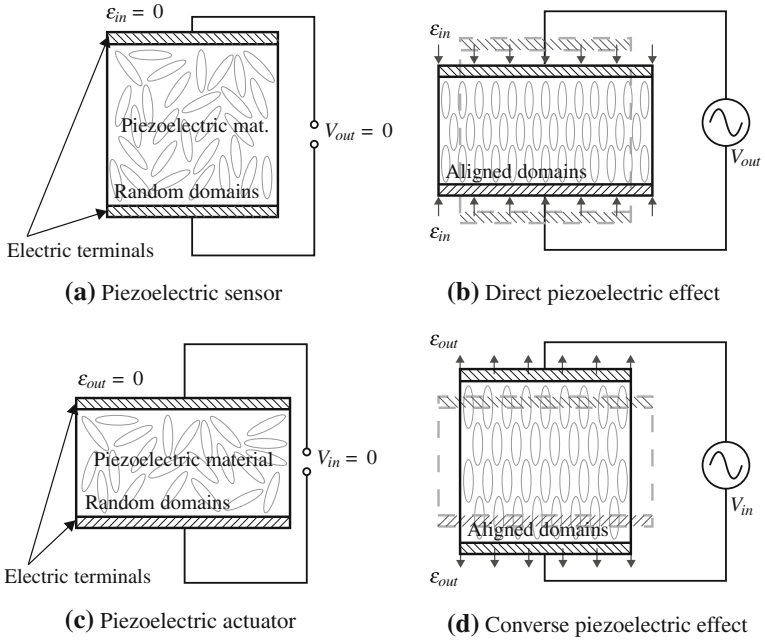

(a) Piezoelectric sensor **(b)** Direct piezoelectric effect

(c) Piezoelectric actuator **(d)** Converse piezoelectric effect

Fig. 3.15 The direct piezoelectric effect, or in other words the piezoelectric material in sensor mode, is illustrated in (**a**) and (**b**). After the application of a deformation to the material causing a strain change, voltage can be measured on the terminal. The reverse of this effect is illustrated in (**c**) and (**d**) where after the application of a voltage, the material deforms

helicopter rotor blades. Forces generated by converse piezoelectricity are enormous, in the order of tens of meganewtons but the small displacement is the reason why this is not so obvious.

From the viewpoint of control, piezoelectric materials have a linear response to the applied voltage [70, 91]. Since piezoceramics have a ferroelectric nature, they can show signs of hysteretic behavior. In fact, the hysteresis of PZT materials is relatively significant and is in the order of 10−15% [91]. In practical terms, *hysteresis* means that the output displacement of the piezoelectric actuator not only depends on the applied voltage, but also depends on how that voltage was applied previously. Hysteresis manifests mainly with high voltage drives, although in scenarios where the actuator is driven by low voltage amplifiers this effect may be practically neglected [32, 48, 70]. The presence of hysteresis may have an effect on stability and closed-loop performance [70, 129]. This type of actuator nonlinearity is mainly important in control systems where the piezoelectric transducers are used to position an object precisely, for example AFM scanning probes [56, 111]. Such quasi-static application fields may utilize a closed-loop compensation of hysteresis, but the use of such techniques in combination with dynamic systems is discouraged, since it may lead to instability [91]. The hysteresis effect in piezoceramic materials and techniques

overcoming it are discussed in the book by Moheimani and Fleming [70]. In addition to hysteresis, piezoelectric materials may also demonstrate *creep* [21, 95, 129], which is a tendency of the material to slowly move or deform under the effect of a permanent voltage input. Methods aimed at overcoming hysteresis and creep in piezoelectric materials are discussed in [21, 37, 48] and others. The simulations and experiments presented in the upcoming chapters neglect the effect of hysteresis and creep in the piezoelectric transducers, because they are driven by low voltages in a dynamic application scenario.

3.4.2 Piezoelectric Transducers in Vibration Control

The converse piezoelectric effect may be readily utilized in active vibration control as a source of actuation force. At the same time, the direct piezo effect allows to use piezoelectric materials as sensors as well. The availability, price and electromechanical properties of piezoelectric transducers set these devices at the forefront of vibration control applications. Their usage in the field of AVC continues to be popular among both engineering practitioners and researchers.

Because experimental studies aimed at the active vibration control of flexible beams predominantly use piezoceramics as actuating elements, the AVC demonstration device introduced in the upcoming Chap. 5 will also feature piezoelectric actuators. The price range, effectiveness and simplicity of these devices and moreover the possibility to integrate them into active structures renders them as an ideal option for this laboratory application [112, 115]. As a complete review of all possible aspects of the use of piezoceramics in AVC is not in the scope of this work, we will leave the exhausting analysis of modeling techniques, placement optimization aspects and other details to our more experienced colleagues. The available literature on the application of piezoelectric materials, transducer design, placement strategy, types of actuators and their use in vibration control is very broad, we may recommend the excellent books by Fuller et al. [33] and many others [9, 45, 87].

The use of piezoelectric patches for the vibration control of cantilever beams [64, 97, 113, 114, 127] and plates [16, 59, 63] is especially popular in the literature and there is an abundance of publications on the topic of these demonstrative examples. Piezoelectric patches have been suggested for use on systems with dynamics similar to vibrating beams, such as on robotic manipulators arms [98, 124, 132] and satellite boom structures [74]. Further real-life examples of piezoceramics in vibration control are scanning position tables, scanning probe microscopes such as the atomic force microscope (AFM), magnetic force microscope (MFM), micropositioning platforms [29, 60], or the vibration attenuation of civil engineering structures [102]. Less common engineering applications of piezoelectric actuators in AVC are for example the vibration control of grinding machines proposed by Albizuri et al. [2], vibration suppression in gantry machines as proposed by Stöppler in [106], vibration damping of car body structures [52] and gearboxes [40], and aeroelastic wing control [108].

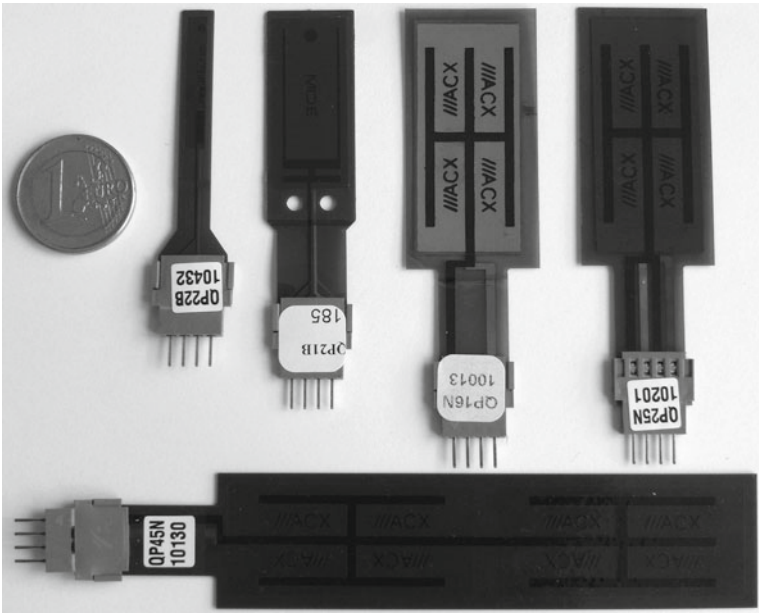

Fig. 3.16 A range of commercial piezoelectric transducers in different shape and size variations, contrasted to the 1 Euro coin for size reference

Figure 3.16 illustrates a range of commercially produced piezoelectric transducers. A wide selection of transducer shape and size configurations is currently available on the market, moreover they can be manufactured according to the needs of the customer. The transducers shown in the figure come in a pre-packaged form with the necessary electric leads bonded on the surface, equipped with a protective foil and a connection terminal. The longer transducer pictured at the bottom (marked as QP45N) and the transducer on the right (marked as QP25N) contain two layers of piezoceramics. These two layers can be used either with the same input signal to achieve larger actuation force or one layer can be utilized as an actuator while the other as sensor to achieve near perfect collocation.

3.4.3 Mathematical Description of the Piezoelectric Effect

The relative expansion or strain of a piezoelectric element is proportional to the applied field strength. It may be calculated very simply, by using the following formula [88]:

$$\varepsilon = \frac{\triangle l}{l_0} d_{ij} E \tag{3.7}$$

$$E = \frac{U}{w_s} \tag{3.8}$$

where d_{ij} is the piezoelectric constant of the material, E is the electric field strength, U the applied voltage and finally w_s is the thickness of the piezoelectric material in the poling direction. The electric behavior of the material is described by

$$\mathbf{D_e} = \varepsilon_\sigma \mathbf{E_e} \tag{3.9}$$

where $\mathbf{D_e}$ is the electric displacement, ε_σ is permittivity and $\mathbf{E_e}$ is the electric field strength. Similarly, the mechanical properties are described by Hooke's law:

$$\mathbf{S} = \mathbf{s}_E \sigma \tag{3.10}$$

where $\mathbf{S}$ is strain, $\mathbf{s}_E$ is the compliance matrix and σ is stress. When we combine these two equations, we obtain the coupled piezoelectric equations in the strain-charge form [33, 87]:

$$\mathbf{S} = \mathbf{s}_E \sigma + \mathbf{d}^T \mathbf{E_e} \tag{3.11}$$

$$\mathbf{D_e} = \mathbf{d}\sigma + \varepsilon_\sigma \mathbf{E_e} \tag{3.12}$$

where $\mathbf{d}$ represents the piezoelectric coupling constants. Subscripts $_E$ indicate zero (or constant) electric field and $_\sigma$ zero (or constant) stress field. Superscript ^{T} denotes matrix transposition. Equation (3.11) may be used to express relations for a piezoelectric actuator and similarly (3.12) is used to describe the behavior of a piezoelectric sensor. For additional clarity, these equations can be expressed for a poled piezoelectric ceramic like PZT in the following form:

$$\begin{bmatrix} S_1 \\ S_2 \\ S_3 \\ S_4 \\ S_5 \\ S_6 \end{bmatrix} = \begin{bmatrix} s_{11}^E & s_{12}^E & s_{13}^E & 0 & 0 & 0 \\ s_{12}^E & s_{11}^E & s_{13}^E & 0 & 0 & 0 \\ s_{13}^E & s_{13}^E & s_{33}^E & 0 & 0 & 0 \\ 0 & 0 & 0 & s_{44}^e & 0 & 0 \\ 0 & 0 & 0 & 0 & s_{44}^e & 0 \\ 0 & 0 & 0 & 0 & 0 & s_{66}^e \end{bmatrix} \begin{bmatrix} \sigma_1 \\ \sigma_2 \\ \sigma_3 \\ \sigma_4 \\ \sigma_5 \\ \sigma_6 \end{bmatrix} + \begin{bmatrix} 0 & 0 & d_{31} \\ 0 & 0 & d_{31} \\ 0 & 0 & d_{31} \\ 0 & d_{15} & 0 \\ d_{15} & 0 & 0 \\ 0 & 0 & 0 \end{bmatrix} \begin{bmatrix} E_1 \\ E_2 \\ E_3 \end{bmatrix} \tag{3.13}$$

$$\begin{bmatrix} D_1 \\ D_2 \\ D_3 \end{bmatrix} = \begin{bmatrix} 0 & 0 & 0 & 0 & d_{15} & 0 \\ 0 & 0 & 0 & d_{15} & 0 & 0 \\ d_{31} & d_{31} & d_{33} & 0 & 0 & 0 \end{bmatrix} \begin{bmatrix} \sigma_1 \\ \sigma_2 \\ \sigma_3 \\ \sigma_4 \\ \sigma_5 \\ \sigma_6 \end{bmatrix} + \begin{bmatrix} \varepsilon_{11} & 0 & 0 \\ 0 & \varepsilon_{11} & 0 \\ 0 & 0 & \varepsilon_{33} \\ 0 & 0 & 0 \end{bmatrix} \begin{bmatrix} E_1 \\ E_2 \\ E_3 \end{bmatrix} \tag{3.14}$$

The previous equation makes use of the crystal symmetry, thus showing only the relevant elements in the matrices. Naturally, for other fundamental types of piezoelectric materials these matrices are in a different form. The elements d_{ij} of the matrix d express the coupling between the electric field in the i direction and the strain in the j direction. In practice, due to crystal symmetries, the coupling matrix d has only a few non-zero elements.

3.4.4 FEM Formulation for Piezoelectric Transducers

The previously introduced Eqs. (3.11) and (3.12) provide the basis for the finite element (FE) formulation of an engineering problem involving a structure with piezoelectric actuators. The approach is similar to the modeling of lumped parameter mechanical systems introduced in Sect. 2.4, with both the mechanical and the electrical terms in the equation of motion. Analogies between the structural damping and dielectric loss, furthermore in between the stiffness / permittivity / coupling are made use of when formulating the underlying set of equations expressed in the following matrix form:

$$\begin{bmatrix} \mathbf{M} & \mathbf{0} \\ \mathbf{0} & \mathbf{0} \end{bmatrix} \begin{bmatrix} \ddot{\mathbf{q}} \\ \ddot{\mathbf{p}} \end{bmatrix} + \begin{bmatrix} \mathbf{B_d} & \mathbf{0} \\ \mathbf{0} & \mathbf{B_p} \end{bmatrix} \begin{bmatrix} \dot{\mathbf{q}} \\ \dot{\mathbf{p}} \end{bmatrix} + \begin{bmatrix} \mathbf{K_s} & \mathbf{K_z} \\ \mathbf{K_z}^T & \mathbf{K_p} \end{bmatrix} \begin{bmatrix} \mathbf{q} \\ \mathbf{p} \end{bmatrix} = \begin{bmatrix} \mathbf{f}_e \\ \mathbf{L_e} \end{bmatrix} \tag{3.15}$$

where $\mathbf{B_d}$ is responsible for structural damping, $\mathbf{B_p}$ for dielectric loss and $\mathbf{M}$ is a mass matrix. Terms $\mathbf{q}$ and $\mathbf{p}$ and their first and second order derivatives express the structural and electrical degrees of freedom. $\mathbf{K_p}$ is anisotropic permittivity, $\mathbf{K_s}$ is the anisotropic stiffness and finally $\mathbf{K_z}$ and is responsible for coupling—or simply stated, the piezoelectric effect.

The above formulation, familiar from lumped parameter vibrating systems is formulated for piezoelectrics using the stress–charge form of the piezoelectric equations, which are given by

$$\begin{aligned} \sigma &= \mathbf{c}_E \mathbf{S} - \mathbf{e_p} \mathbf{E_e} \\ \mathbf{D_e} &= \mathbf{e_p}^T \mathbf{S} + \varepsilon_S \mathbf{E_e} \end{aligned} \tag{3.16}$$

where $\mathbf{e_p}$ are the piezoelectric coupling coefficients in the stress–charge form, $\mathbf{c}_E$ contains stiffness coefficients under constant electric field and ε_S is the electric permittivity matrix under constant stain. As we can see, this equation differs considerably from (3.11) and (3.12), which are given in the strain–charge form. Other representations of the linear piezoelectric equations are also possible, as we can express the constitutive equations in stress–charge, strain–charge, strain–voltage and stress–voltage forms.

Although the FEM representation of the piezoelectric effect is based on the stress–charge form using the $\mathbf{e_p}$ coupling term, the piezoelectric matrix $\mathbf{d}$ can also be directly used and defined in most FEM packages. For example in the ANSYS package, $\mathbf{d}$ is defined in the strain–charge matrix form. This is then internally converted into the piezoelectric stress–charge matrix, using the strain matrix at a constant temperature. Conversion between the strain charge to stress charge is calculated according to [44]:

$$\varepsilon_S = \varepsilon_\sigma - \mathbf{d}\mathbf{s}_E^{-1}\mathbf{d}^T \tag{3.17}$$

$$\mathbf{e_p} = \mathbf{d}\mathbf{s}_E^{-1} \tag{3.18}$$

$$\mathbf{c_E} = \mathbf{s}_E{}^{-1} \tag{3.19}$$

where subscripts $_\sigma$, $_S$, $_E$ indicate that the values were evaluated under a constant stress, strain and electric field. The elements of the anisotropic elasticity matrix may also be expressed by the following terms:

$$\mathbf{s}_E = \begin{bmatrix} \frac{1}{E_x} & -\frac{\nu_{xy}}{E_x} & -\frac{\nu_{xz}}{E_x} & 0 & 0 & 0 \\ 0 & \frac{1}{E_y} & 0 & 0 & 0 & 0 \\ 0 & 0 & \frac{1}{E_z} & 0 & 0 & 0 \\ 0 & 0 & 0 & \frac{1}{G_{xy}} & 0 & 0 \\ 0 & 0 & 0 & 0 & \frac{1}{G_{yz}} & 0 \\ 0 & 0 & 0 & 0 & 0 & \frac{1}{G_{xz}} \end{bmatrix} \qquad G_{xy} = \frac{1}{2[s_{11}^E] - [s_{11}^E]} \tag{3.20}$$

where ν_{xz} is Poisson's ratio in a given direction.

The piezoelectric constitutive equations of (3.16) can also be compacted to a matrix term:

$$\begin{bmatrix} \sigma \\ \mathbf{D} \end{bmatrix} = \begin{bmatrix} \mathbf{c}_E & \mathbf{e_p} \\ \mathbf{e_p}{}^T & -\varepsilon_S \end{bmatrix} \begin{bmatrix} \mathbf{S} \\ -\mathbf{E} \end{bmatrix} \tag{3.21}$$

After applying the variational principle and finite element discretization, one will arrive at the form introduced by (3.15). The damping matrix $\mathbf{B_p}$ responsible for the dielectric loss will contain the negative element dielectric damping matrix, $\mathbf{K_p}$ will contain the negative element dielectric permittivity coefficient matrix and $\mathbf{K_z}$ the piezoelectric matrix [3].

A finite element formulation of a vibrating beam may be created using the Euler Bernoulli model, where the beam section with piezo patches is considered to be laminated and the rest isotropic [36]. The numerical model of Gaudenzi et al. contains not only the mechanic and piezoelectric parts - but also the electronic components like the voltage amplifier.

A practical guide to simulating the electromechanical behavior of a transversally vibrating beam equipped with piezoelectric transducers is given in Appendix. A for those interested. The text lists an ANSYS code with a detailed description of the commands and the process of creating a working model.

3.5 Electrochemical Materials

Electroactive polymers (EAP) are artificial polymer-based smart materials reacting to applied electric current through a change in size. The coupling is electro-mechanical just like in the case of piezoceramic materials. While the normal piezoelectric materials may exhibit large forces, their percentual elongation is typically in the order of mere 0.1%. However, for certain types of EAP this can be more than 300% [11, 131]. Electroactive polymers can be divided into two fundamental classes:

- dielectric
- ionic

3.5.1 Dielectric EAP

In dielectric or "dry" EAP, actuation is caused by electrostatic forces [10]. Dielectric EAP materials work like a capacitor: due to the introduced electrical field the capacitance changes and the actuator compresses in thickness and expands in area. Typically, dielectric EAP actuators exhibit large strains, albeit they require a large actuating voltage in the range of hundreds or even thousands of volts. This type of EAP requires no electrical power to keep the actuator at the desired position.

The most common type of dielectric EAP material is polyvinylidene fluoride (PVDF), which is a part of the ferroelectric polymer family.[10] Electrostatic fields in the range of 200 MV/m can induce strains of 2%, which exceeds the capability of piezoceramics. In addition to the large actuating voltages, the applied electric field in PVDF is also very close to the breakdown potential of the material. Ferroelectric polymers are not to be confused with ferroceramics. The piezoelectric effect is linear and reversible, however electrostriction in PVDF is only one way and nonlinear.

Electro-statically stricted polymer (ESSP) actuators are made from polymers with low elastic stiffness and high dielectric constants. These polymers are then subjected to an electrostatic field to induce deformation. The most common physical configuration of ESSP are rope-like longitudinal or bending type actuators. A very large actuation potential in the range of 100 V/μm is required to induce strains in the order of 10–200%. Moreover, these excessive voltages are very close to the breakdown potential of the material, therefore in practice they have to be lowered. Thin actuators of less than 50 μm are used to decrease the required actuation voltage. Similar to the polarization limits of piezoceramics, different types of EAP also require constraints on the input voltage. An effective way to include these constraints into the controller (while maintaining the stability of the resulting nonlinear control law and full performance optimality) is the application of the model predictive control strategy.

Electro-viscoelastic elastomers (EVE) are a type of dielectric EAP that are closely related to magnetorheological fluids. In fact, before a curing process, EVE behave analogously to MR fluids. The difference between the two types of materials is introduced with a curing cycle, when an electric field is applied to fix in the position of the polar phase in the elastomer. EVE materials can be used as an alternative to MR fluids in vibration control systems [10].

According to the experiments by Palakodeti and Kessler, the relative increase in area of dielectric EAP is roughly linearly dependent on the applied electric field [84]. The highest actuator efficiency has been measured at the largest prestrain and smallest frequency values, while a frequency of 20 Hz caused an efficiency drop to 25%.

---

[10] Due to the inherent similarities with piezoceramic materials, sometimes polyvinylidene fluoride (PVDF) is regarded to be a piezoelectric material. The piezoelectric effect is reversible, however the actuating effect in PVDF is only one way.

3.5.2 Ionic EAP

In ionic EAP, actuation is caused by the diffusion and subsequent displacement of ions. The driving chemical reaction in ionic EAP is a change from an acid to a base environment, in other words the ionic EAP materials have fixed anions and mobile cations [7]. This reaction can be stimulated electrically with embedded electrodes [19]. Upon the application of electric current, the cathode becomes basic while the anode acidic—the cations begin to migrate towards the electrodes. Unfortunately, the response time is slow due to the need of the ions to diffuse through the material, and the electrodes degrade very rapidly. For example in the work of Calvert et al. the swelling of an ionic EAP gel structure to twice its original size took approximately 20 min, while the process could only be repeated 2–3 times due to the chemical degradation of electrodes [19]. Depending on thickness and the kinetics of the chemical reaction, other materials can exhibit actuation changes measured in milliseconds to minutes [10]. While much lower actuation voltages are needed in ionic EAP, larger electrical current is required to start and maintain the ionic flow within the material. The disadvantage is that power is also required to keep the actuator at a given position. Actuators made from ionic EAP are predominantly bending type structures [11]. Due to its fundamental working principle, ionic EAP are also referred to as "wet" EAP [10].

Perfluorinated ion exchange membrane platinum composite (IPMC) treated with an ionic salt and deposited with electrodes on both sides is a common type of ionic EAP material often cited in the literature and utilized in academic research. The ionic base polymer used to create IPMC is typically 200 μm thick [55], and it is available under the market names Nafion or Flemion [4, 31]. IPMC actuated with low voltages in the range of 1–10 V demonstrates large displacements in the sub 0.1 Hz frequency range. Unfortunately, the displacement response decreases very rapidly with increased frequencies [10]. An application of voltages above 1 V induces electrolysis; causing degradation, heat and gas generation. The schematic of the electro-mechanical behavior of an IPMC-based ionic EAP actuator is illustrated in Fig. 3.17.

Carbon nanotubes are another emerging type of ionic EAP actuators. As the name implies, these materials consists of two narrow sheets of carbon nanotubes bonded together through an electrically insulated adhesive layer. This composite structure is then immersed in an electrolyte. Carbon nanotube EAP can achieve strains in the order of 1% [10]. In addition to the usual disadvantages of wet EAP materials, carbon nanotube-based EAP are expensive and their mass production is difficult as well.

As of today, the commercial availability and acceptance of EAP materials is still very limited, most of the EAP research projects utilize custom made materials and actuators. The main limitations of EAP are low actuation forces, lack of robustness and no well-established commercial material types with guaranteed properties. Ionic EAP requires protective coatings to maintain moisture continuously within the material [8]. Bending type structures are the most convenient to manufacture and while the shape change is very easily induced, the actuating forces are weak.

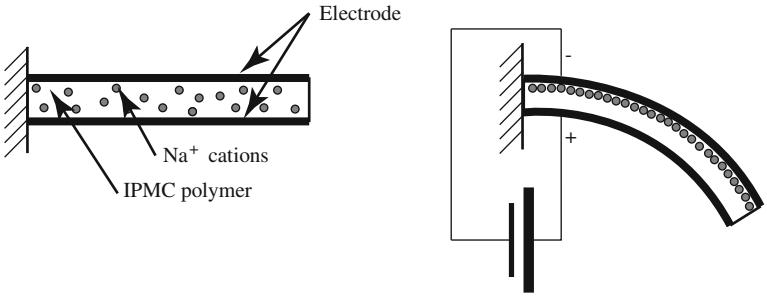

Fig. 3.17 Mechanical behavior of an IPMC based ionic EAP actuator

3.5.3 EAP in Vibration Control

Generally, the use of EAP in active vibration control applications cannot be recommended. This is due to the above-mentioned disadvantages such as the lack of robustness or the technical readiness, availability or acceptance of EAP materials. In addition to that, the effective bandwidth and internal chemical degradation or electrode corrosion makes the use of EAP in vibration control somewhat limited. Recent interest of the scientific and engineering community gives hope for the further progress of the development of electroactive polymers. A more mature EAP technology is certainly a good basis for practical applications in active vibration damping.

Passive structural vibration damping via EAP materials is possible and limited research exists in the field. The damping properties of carbon nanotube EAP enforced structures are for example discussed in [93], while other researchers are examining the passive vibration damping provided by deposited layer of electroactive polymers [66]. Only a handful of academic publications deal with the use of EAP as possible actuators in vibration control. Space mission vibration control through IPMC-based ionic EAP has been suggested without detailed elaboration in [53] by Krishen et al. This is of course only possible with very low bandwidth actuation of large and flexible structures in the sub Hertz range.

An earlier work discusses IPMC-based active vibration control in more detail: the tip of a flexible link has been stabilized by Bandopadhya et al. using ICMP patches controlled by distributed PD controllers [7]. Here EAP is considered instead of piezoceramics because of the lower actuation voltage and the lack of brittleness. It is interesting to note that according to Bandopadhya et al. in addition to the voltage and bending curvature the voltage bending moment relationship remains linear for the considered IPMC material. Moreover, experimental results suggest that, if piezo patches are used as sensors on an IPMC actuated bimorph, the generated voltage is proportional to the tip deflection [8]. The experimental evaluation in this work utilizes a 2 Hz excitation signal, it however demonstrates only a 1 second time response showing the vibration in a higher order mode around 50 Hz. It is unclearwhether

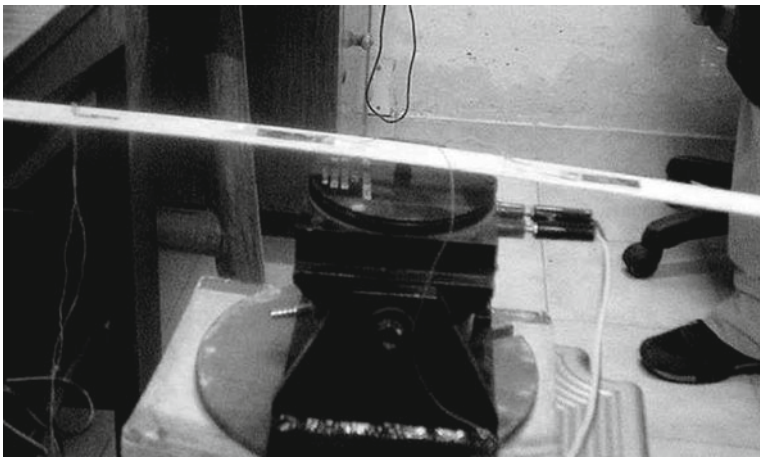

Fig. 3.18 Experimental vibration control setup using electroactive polymer actuators [7, 8]

the vibration damping is due to the active effect of the EAP enabled beam or the damping would even be present with activated EAP patches in a semi-active fashion. The experimental vibration control setup used by Bandopadhya et al., which features electroactive polymer actuators is shown[11] in Fig. 3.18.

Attempts to model the electro-mechanical dynamics of EAP actuators mathematically have been discouraged by the complexity of the task and the several unknown factors such as the humidity in ionic EAP, static prestrain, manufacturing irregularities and other environmental factors. Other challenges in the modeling of EAP include nonlinearity,[12] large mechanical compliance (mismatch between the properties of the material and electrodes), hysteresis and non-homogeneity of the material resulting from the manufacturing process [12]. It is more of an experimental approach, however we must note the work of Lavu et al. in which the authors developed an observer Kalman filter identification (OKID) based state-space multi-model for IPMC taking into account the relative humidity around the actuator [55].

3.6 Other Types of Materials and Actuators

There are several other types of smart materials that have not been explicitly discussed here. These include chemically activated polymers, light-activated materials, magnetically or thermally activated polymers and gels [11].

If an electrically conductive material is subjected to a time-changing magnetic field, eddy currents are formed in the conductor. The eddy currents circulate within the

[11] Courtesy of Bishakh Bhattacharya.

[12] As some researchers have pointed out through experimental tests, models could be linearized as EAP behaves linearly under certain conditions [8, 84].

conductor creating an inside magnetic field which is then mutually interacting with the outside magnetic field thus creating dynamic forces between the conductor and the field. Utilizing this effect, an electromagnet placed in the vicinity of a conductor can be used as an actuator to attenuate vibrations. According to Sodano and Inman, the first use of an active eddy current actuator for vibration suppression is demonstrated in [100]. Eddy current dampers are suggested for the vibration control of a cantilever beam earlier in [6], while Gospodarič et al. used a pair of electromagnets to control vibrations in a ferromagnetic cantilever beam in [39] as well. In a more traditional approach, a mechanical structure can be actuated by simply placing an electromagnet close to its surface and using the magnetic forces between the ferromagnetic materials or permanent magnets and the actuating coil as means of actuation. In this case, the coupling between the electric and magnetic effect is indirect, and we cannot speak of smart materials. For example, a cantilever beam is actuated by an electromagnet placed underneath the beam tip in the work of Fung et al. [34].

This chapter has been mainly concerned with the use of smart materials as actuators or sensors. However, vibrating mechanical systems are often actuated through traditional actuators such as linear motors or hydraulic devices. An electrodynamic shaker is directly utilized as an actuator for the vibration control of a robotic arm by Dadfarnia et al. in [30]. A two degree of freedom mass-spring-damper demonstration device is actuated using a hydraulic piston in a work by VandenBroeck et al. [118, 119].

References

1. Active Materials Laboratory, UCLA (2010) Magnetostriction and magnetostrictive materials. Online, http://aml.seas.ucla.edu/research/areas/magnetostrictive/mag-composites%/Magnetostriction%20and%20Magnetostrictive%20Materials.htm
2. Albizuri J, Fernandes M, Garitaonandia I, Sabalza X, Uribe-Etxeberria R, Hernández J (2007) An active system of reduction of vibrations in a centerless grinding machine using piezoelectric actuators. Int J Mach Tools Manuf 47(10):1607–1614. doi:10.1016/j.ijmachtools.2006.11.004, http://www.sciencedirect.com/science/article/B6V4B-4MR1K43-1/2/aa1014dd203b27a44c75cef37a2adf09
3. Ansys Inc (2009) Release 12.1 Documentation for ANSYS. Ansys Inc. / SAS IP Inc., Canonsburg
4. Asahi Glass (2010) Flemion: a fluoropolymer ion-exchange membrane which protects global environment through outstanding technologies. Tokyo. Online, http://www.agc.com/english/csr/environment/products/positive_seihin5.html
5. Aslam M, Xiong-Liang Y, Zhong-Chao D (2006) Review of magnetorheological (MR) fluids and its applications in vibration control. J Marine Sci Appl 5(3):17–29
6. Bae JS, Kwak MK, Inman DJ (2005) Vibration suppression of a cantilever beam using eddy current damper. J Sound Vib 284(3–5):805–824. doi:10.1016/j.jsv.2004.07.031, http://www.sciencedirect.com/science/article/B6WM3-4F1J8KP-D/2/f6ceedf67a74bb2aadd57e99f8bea787
7. Bandopadhya D, Bhogadi D, Bhattacharya B, Dutta A (2006) Active vibration suppression of a flexible link using ionic polymer metal composite. In: 2006 IEEE conference on robotics, automation and mechatronics, pp 1–6. doi:10.1109/RAMECH.2006.252638

8. Bandopadhya D, Bhattacharya B, Dutta A (2007) An active vibration control strategy for a flexible link using distributed ionic polymer metal composites. Smart Mater Struct 16(3):617. http://stacks.iop.org/0964-1726/16/i=3/a=008
9. Bandyopadhyay B, Manjunath T, Umapathy M (2007) Modeling, control and implementation of smart structures: A FEM-State Space Approach, 1st edn. Springer, Berlin
10. Bar-Cohen Y (2000) Electroactive polymers as artificial muscles —capabilities, potentials and challenges, 1st edn, NTS Inc., Chap 8.11, pp 936–950. Handbook on Biomimetics
11. Bar-Cohen Y (2002) Electro-active polymers: current capabilities and challenges. In: Proceedings of the SPIE smart structures and materials symposium, San Diego, pp 4695–4702
12. Bar-Cohen Y, Sheritt S, Lih SS (2001) Electro-active polymers: current capabilities and challenges. In: Proceedings SPIE 8th annual international symposium on smart structures and materials, Newport, pp 4329–4343
13. Bars R, Colaneri P, de Souza CE, Dugard L, Allgöwer F, Kleimenov A, Scherer C (2006) Theory, algorithms and technology in the design of control systems. Annu Rev Control 30(1):19–30. doi:10.1016/j.arcontrol.2006.01.006, http://www.sciencedirect.com/science/article/B6V0H-4K7WTXH-1/2/705feea29964327e5fd83768ae0f99e2, 2005 IFAC Milestone Reports
14. Bartlett P, Eaton S, Gore J, Metheringham W, Jenner A (2001) High-power, low frequency magnetostrictive actuation for anti-vibration applications. Sens Actuators A 91(1–2):133–136. doi:10.1016/S0924-4247(01)00475-7, http://www.sciencedirect.com/science/article/B6THG-4313YT1-14/2/851ac15043a568a17313eef3042d685f, Third European Conference on Magnetic Sensors & Actuators.
15. Baz A, Imam K, McCoy J (1990) Active vibration control of flexible beams using shape memory actuators. J Sound Vib 140(3):437–456. doi:10.1016/0022-460X(90)90760-W, http://www.sciencedirect.com/science/article/B6WM3-494TCC5-NS/2/7f451727d377dc9c69f873e2c0d85665
16. Birman V, Adali S (1996) Vibration damping using piezoelectric stiffener-actuators with application to orthotropic plates. Compos Struct 35(3):251–261, doi:10.1016/0263-8223(96)00011-6. http://www.sciencedirect.com/science/article/B6TWP-3VS925W-1/2/a20cdc4439f3d1f8f958988ad0b645f3
17. Bouzidane A, Thomas M (2008) An electrorheological hydrostatic journal bearing for controlling rotor vibration. Comput Struct 86(3–5):463–472. doi:10.1016/j.compstruc.2007.02.006, http://www.sciencedirect.com/science/article/B6V28-4NDVGTG-1/2/32b829850e8db109469179cdb7d7d4f6, Smart Structures
18. Braghin F, Cinquemani S, Resta F (2010) A model of magnetostrictive actuators for active vibration control. Sens Actuators A (in press) Corrected Proof:–, doi:10.1016/j.sna.2010.10.019, http://www.sciencedirect.com/science/article/B6THG-51F25N5-4/2/f5cf46980d38877c74a3c4d34fbd894d
19. Calvert P, O'Kelly J, Souvignier C (1998) Solid freeform fabrication of organic-inorganic hybrid materials. Mater Sci Eng C 6(2–3):167–174. doi:10.1016/S0928-4931(98)00046-0, http://www.sciencedirect.com/science/article/B6TXG-3W0G7X7-B/2/6975c02114a4ef48788129ec9b336c73
20. CEDRAT Group (2009) Magnetostrictive actuator prototypes and FEM simulation. Meylan Cedex. Online, http://www.cedrat.com/en/technologies/actuators/magnetic-actuators-motors.html
21. Changhai R, Lining S (2005) Hysteresis and creep compensation for piezoelectric actuator in open-loop operation. Sens Actuators A 122(1):124–130. doi:10.1016/j.sna.2005.03.056, http://www.sciencedirect.com/science/article/pii/S0924424705001512, sSSAMW 04 - Special Section of the Micromechanics Section of Sensors and Actuators based on contributions revised from the Technical Digest of the 2004 Solid-State Sensor, Actuator and Microsystems Workshop
22. Chen Q, Levy C (1999) Vibration analysis of flexible beam by using smart damping structures. Composites Part B: Eng 30:395–406

23. Choi SB, Hwang JH (2000) Structural vibration control using shape memory actuators. J Sound Vib 231(4):1168–1174. doi:10.1006/jsvi.1999.2637, http://www.sciencedirect.com/science/article/B6WM3-45CWW19-HC/2/a61f7091ea2a3e8325d72991c1da1b04
24. Choi SB, Han YM, Kim JH, Cheong CC (2001) Force tracking control of a flexible gripper featuring shape memory alloy actuators. Mechatronics 11(6):677–690, doi:10.1016/S0957-4158(00)00034-9, http://www.sciencedirect.com/science/article/B6V43-43MMSYG-6/2/cec92f6a51314ef45e91c5caf9e5859e
25. Choi SB, Hong SR, Sung KG, Sohn JW (2008) Optimal control of structural vibrations using a mixed-mode magnetorheological fluid mount. Int J Mech Sci 50(3):559–568. doi:10.1016/j.ijmecsci.2007.08.001, http://www.sciencedirect.com/science/article/B6V49-4PD4XHC-1/2/c491dc4a4a881e38b0e20ceef7206dec
26. Choy S, Jiang X, Kwok K, Chan H (2010) Piezoelectric and dielectric characteristics of lead-free BNKLBT ceramic thick film and multilayered piezoelectric actuators. Ceram Int 36(8):2345–2350. doi:10.1016/j.ceramint.2010.07.030, http://www.sciencedirect.com/science/article/B6TWH-50P9H3H-T/2/b62d4dee5b14f6a8678c3fc747ae42e8
27. Clark A, Savage H, Spano M (1984) Effect of stress on the magnetostriction and magnetization of single crystal Tb.27Dy.73Fe2. IEEE Trans Magn 20(5):1443–1445. doi:10.1109/TMAG.1984.1063469
28. Corbi O (2003) Shape memory alloys and their application in structural oscillations attenuation. Simul Modell Pract Theory 11(5–6):387–402. doi:10.1016/S1569-190X(03)00057-1, http://www.sciencedirect.com/science/article/B6X3C-49097BD-1/2/70ef399b2b05b43d6182b568e028b58c, Modeling and Simulation of Advanced Problems and Smart Systems in Civil Engineering
29. Cunningham M, Jenkins D, Clegg W, Bakush M (1995) Active vibration control and actuation of a small cantilever for applications in scanning probe instruments. Sens Actuators A 50(1–2):147–150. doi:10.1016/0924-4247(96)80099-9, http://www.sciencedirect.com/science/article/B6THG-3YVM62R-15/2/ea100dfeea242e7471472799494a5b93
30. Dadfarnia M, Jalili N, Liu Z, Dawson DM (2004) An observer-based piezoelectric control of flexible cartesian robot arms: theory and experiment. Control Eng Pract 12(8):1041–1053. doi:10.1016/j.conengprac.2003.09.003, http://www.sciencedirect.com/science/article/B6V2H-49WMRJ4-4/2/eb147ee81930b34eb0aba81e90b3a711, Special Section on Emerging Technologies for Active Noise and Vibration Control Systems
31. DuPont (2010) Nafion membranes. Wilmington. Online, http://www2.dupont.com/Automotive/en_US/products_services/fuelCell/nafion.html
32. Fuller C (1990) Active control of sound transmission/radiation from elastic plates by vibration inputs: I. analysis. J Sound Vib 136(1):1–15. doi:10.1016/0022-460X(90)90933-Q, http://www.sciencedirect.com/science/article/pii/0022460X9090933Q
33. Fuller CR, Elliott SJ, Nelson PA (1996) Active Control of Vibration, 1st edn. Academic Press, San Francisco
34. Fung RF, Liu YT, Wang CC (2005) Dynamic model of an electromagnetic actuator for vibration control of a cantilever beam with a tip mass. J Sound Vib 288(4–5):957–980. doi:10.1016/j.jsv.2005.01.046, http://www.sciencedirect.com/science/article/B6WM3-4G4N5VD-1/2/fc3710f0625ef69f19d16c8778a63e58
35. Ganilova O, Cartmell M (2010) An analytical model for the vibration of a composite plate containing an embedded periodic shape memory alloy structure. Compos Struct 92(1):39–47. doi:10.1016/j.compstruct.2009.06.008, http://www.sciencedirect.com/science/article/B6TWP-4WMDHPH-1/2/5c0b8fba0f2e05dad5142ddfcbc48f32
36. Gaudenzi P, Carbonaro R, Benzi E (2000) Control of beam vibrations by means of piezoelectric devices: theory and experiments. Compos Struct 50:373–379
37. Gaul L, Becker J (2009) Model-based piezoelectric hysteresis and creep compensation for highly-dynamic feedforward rest-to-rest motion control of piezoelectrically actuated flexible structures. Int J Eng Sci 47(11–12):1193–1207. doi:10.1016/j.ijengsci.2009.07.006, http://www.sciencedirect.com/science/article/pii/S0020722509001219, Mechanics, Mathematics

and Materials a Special Issue in memory of A.J.M. Spencer FRS—In Memory of Professor A.J.M. Spencer FRS
38. Giannopoulos G, Santafe F, Vantomme J, Buysschaert F, Hendrick P (2006) Smart helicopter blade using piezoelectric actuators for both cyclic and collective pitch control. Multifunctional Structures / Integration of Sensors and Antennas 11(1)
39. Gospodaric B, Voncina D, Bucar B (2007) Active electromagnetic damping of laterally vibrating ferromagnetic cantilever beam. Mechatronics 17(6):291–298. doi:10.1016/j.mechatronics.2007.04.002, http://www.sciencedirect.com/science/article/B6V43-4NVSWV6-1/2/5c4672945cfa9b81238f0b1cb8a8eb13
40. Guan YH, Lim TC, Shepard WS (2005) Experimental study on active vibration control of a gearbox system. J Sound Vib 282(3–5):713–733. doi:10.1016/j.jsv.2004.03.043, http://www.sciencedirect.com/science/article/B6WM3-4DHXFPJ-4/2/e98625c6c04fd1f5bb5712eb31806f54
41. Hong S, Choi S, Lee D (2006) Comparison of vibration control performance between flow and squeeze mode ER mounts: experimental work. J Sound Vib 291(3–5):740–748, doi:10.1016/j.jsv.2005.06.037, http://www.sciencedirect.com/science/article/B6WM3-4H16P3S-C/2/f98734a231c88a1ec1b43024a2a32f2e
42. Hong SR, Choi SB, Han MS (2002) Vibration control of a frame structure using electro-rheological fluid mounts. Int J Mech Sci 44(10):2027–2045. doi:10.1016/S0020-7403(02)00172-8, http://www.sciencedirect.com/science/article/B6V49-47BX3RX-4/2/53a10ce8cbf8dfa679c34e04beb688e4
43. Ibrahim R (2008) Recent advances in nonlinear passive vibration isolators. J Sound Vib 314(3–5):371–452. doi:10.1016/j.jsv.2008.01.014, http://www.sciencedirect.com/science/article/B6WM3-4S0R6TJ-3/2/8168db91488e18ca41869d56de24ca53
44. Efunda Inc (2007) Constitutive transforms of piezo materials. Sunnyvale. Website, available: http://www.efunda.com/materials/piezo/piezo_math/
45. Inman DJ (2006) Vibration with control. Wiley, Chichester
46. Inman DJ (2007) Engineering Vibrations, 3rd edn. Pearson International Education (Prentice Hall), Upper Saddle River
47. Janke L, Czaderski C, Motavalli M, Ruth J (2005) Applications of shape memory alloys in civil engineering structures: overview, limits and new ideas. Mater Struct 38:578–592. doi:10.1007/BF02479550
48. Janocha H, Kuhnen K (2000) Real-time compensation of hysteresis and creep in piezoelectric actuators. Sens Actuators A 79(2):83–89. doi:10.1016/S0924-4247(99)00215-0, http://www.sciencedirect.com/science/article/pii/S0924424799002150
49. John S, Hariri M (2008) Effect of shape memory alloy actuation on the dynamic response of polymeric composite plates. Composites Part A 39(5):769–776. doi:10.1016/j.compositesa.2008.02.005, http://www.sciencedirect.com/science/article/B6TWN-4RV7YMP-1/2/a8402bbfb476e507253cf32aea87cfb8
50. Jung WJ, Jeong WB, Hong SR, Choi SB (2004) Vibration control of a flexible beam structure using squeeze-mode ER mount. J Sound Vib 273(1–2):185–199. doi:10.1016/S0022-460X(03)00478-4, http://www.sciencedirect.com/science/article/B6WM3-49DFFMM-1/2/1255ad59eca53b0c021632de61aef0b8
51. Knight GPM, UCLA Active Materials Lab (2011) Magnetostrictive materials background. Available http://aml.seas.ucla.edu/research/areas/magnetostrictive/overview.htm
52. Kozek M, Benatzky C, Schirrer A, Stribersky A (2011) Vibration damping of a flexible car body structure using piezo-stack actuators. Control Eng Pract 19(3):298–310. doi:10.1016/j.conengprac.2009.08.001, http://www.sciencedirect.com/science/article/B6V2H-4X3MR4Y-2/2/3ef1d868e70c2b6f10fd9412f9c8c1de, Special Section: IFAC World Congress Application Paper Prize Papers
53. Krishen K (2009) Space applications for ionic polymer-metal composite sensors, actuators, and artificial muscles. Acta Astronautica 64(11–12):1160–1166.

doi:10.1016/j.actaastro.2009.01.008, http://www.sciencedirect.com/science/article/B6V1N-4VM2K65-3/2/f8b0b2d64f274154a5eb59da52fbf524
54. Lau K, Zhou L, Tao X (2002) Control of natural frequencies of a clamped-clamped composite beam with embedded shape memory alloy wires. Compos Struct 58(1):39–47. doi:10.1016/S0263-8223(02)00042-9, http://www.sciencedirect.com/science/article/B6TWP-45XTP9W-N/2/07b9a065ac866d8869a4240deb918851
55. Lavu BC, Schoen MP, Mahajan A (2005) Adaptive intelligent control of ionic polymermetal composites. Smart Mater Struct 14(4):466. http://stacks.iop.org/0964-1726/14/i=4/a=002
56. Lee J, Oh Y, Kim T, Choi M, Jo W (2007) Piezoelectric and electromechanical properties of relaxor ferroelectric Pb(Mg1/3Nb2/3)O3(65%)-PbTiO3(35%) thin films observed by scanning force microscopy. Ultramicroscopy 107(10–11):954–957. doi:10.1016/j.ultramic.2007.02.039, http://www.sciencedirect.com/science/article/B6TW1-4NN6TNC-2/2/a15081aabe1d05ba3faaa00f5797e41d. In: Proceedings of the 8th international conference on scanning robe microscopy, sensors and nanostructures
57. Lee JH, Su RK, Lee PK, Lam LC (2002) Semi-active damping device for vibration control of buildings using magnetorheological fluid. In: Anson M, Ko J, Lam E (eds) Advances in Building Technology, Elsevier, Oxford, pp 969–976, doi:10.1016/B978-008044100-9/50122-4, http://www.sciencedirect.com/science/article/B858K-4PCJRKH-47/2/1c6a74db22e114e2cbddec5d173950f8
58. Li H, Liu S, Wen F, Wen B (2007) Study on dynamic of giant magnetostrictive material transducer with spring of nonlinear stiffness. J Mech Sci Technol 21:961–964. doi:10.1007/BF03027077, http://dx.DOI.org/10.1007/BF03027077
59. Li YY, Cheng L, Li P (2003) Modeling and vibration control of a plate coupled with piezoelectric material. Compos Struct 62(2):155–162. doi:10.1016/S0263-8223(03)00110-7, http://www.sciencedirect.com/science/article/B6TWP-48R1WVK-1/2/f0788ece03ae40a5874f11852e927842
60. Liu YT, Fung RF, Huang TK (2004) Dynamic responses of a precision positioning table impacted by a soft-mounted piezoelectric actuator. Precis Eng 28(3):252–260, doi:10.1016/j.precisioneng.2003.10.005, http://www.sciencedirect.com/science/article/B6V4K-4BMCGD0-1/2/a0f54a4367d9a4fa037b99ba4762a3b9
61. LORD Corporation (2006) Magneto-Rheological (MR) Fluid. LORD Corporation, Cary
62. Lu H, Meng G (2006) An experimental and analytical investigation of the dynamic characteristics of a flexible sandwich plate filled with electrorheological fluid. Int J Adv Manuf Technol 28:1049–1055. doi:10.1007/s00170-004-2433-8, http://dx.DOI.org/10.1007/s00170-004-2433-8
63. Luo Y, Xie S, Zhang X (2008) The actuated performance of multi-layer piezoelectric actuator in active vibration control of honeycomb sandwich panel. J Sound Vib 317(3–5):496–513. doi:10.1016/j.jsv.2008.03.047, http://www.sciencedirect.com/science/article/B6WM3-4SJR2GN-1/2/04c4aad317afe74e20e6f5810f689674
64. Mahmoodi SN, Craft MJ, Southward SC, Ahmadian M (2011) Active vibration control using optimized modified acceleration feedback with adaptive line enhancer for frequency tracking. J Sound Vib 330(7):1300–1311. doi:10.1016/j.jsv.2010.10.013, http://www.sciencedirect.com/science/article/B6WM3-51D894K-1/2/25e8ef1bcadb5fd2aa078de4d678c7f4
65. Maleki M, Naei MH, Hosseinian E, Babahaji A (2011) Exact three-dimensional analysis for static torsion of piezoelectric rods. Int J Solids Struct 48(2):217–226. doi:10.1016/j.ijsolstr.2010.09.017, http://www.sciencedirect.com/science/article/B6VJS-513F90C-5/2/96a4ce72adde5d18a1c509ab880cb797
66. Malinauskas A (2001) Chemical deposition of conducting polymers. Polymer 42(9):3957–3972. doi:10.1016/S0032-3861(00)00800-4, http://www.sciencedirect.com/science/article/B6TXW-42C0RR9-1/2/e8084cbb0f228b86a5cc9d061a340e22
67. McManus SJ, St. Clair KA, Boileau P, Boutin J, Rakheja S (2002) Evaluation of vibration and shock attenuation performance of a suspension seat with a semi-active magnetorheological fluid damper. J Sound Vib 253(1):313–327.

doi:10.1006/jsvi.2001.4262, http://www.sciencedirect.com/science/article/B6WM3-45Y1C16-N/2/33a165ac8f2fe7d8fad7bd83d9484957
68. Memory-Metalle GmbH (2010) Infosheet no. 5: The memory effects—an introduction. White paper, Memory-Metalle GmbH, Weil am Rhein. http://www.memory-metalle.de/html/03_knowhow/PDF/MM_05_introduction_e.pdf, available online (1 page)
69. MIDÉ (2007) Shape memory alloy starter kit—reference manual. MIDÉ Technology, Medford
70. Moheimani S, Fleming AJ (2006) Piezoelectric transducers for vibration control and damping. Springer, London
71. Monkman GJ (1995) The electrorheological effect under compressive stress. J Phys D: Appl Phys 28(3):588. http://stacks.iop.org/0022-3727/28/i=3/a=022
72. Monkman GJ (1997) Exploitation of compressive stress in electrorheological coupling. Mechatronics 7(1):27–36. doi:10.1016/S0957-4158(96)00037-2, http://www.sciencedirect.com/science/article/B6V43-3WDCFB7-3/2/00d7c7757dd73812cfe88867f704ba25
73. Moon SJ, Lim CW, Kim BH, Park Y (2007) Structural vibration control using linear magnetostrictive actuators. J Sound Vib 302(4–5):875–891. doi:10.1016/j.jsv.2006.12.023, http://www.sciencedirect.com/science/article/B6WM3-4N2M6HH-5/2/417522adfca8640acfa76e890ae0533c
74. Moshrefi-Torbati M, Keane A, Elliott S, Brennan M, Anthony D, Rogers E (2006) Active vibration control (AVC) of a satellite boom structure using optimally positioned stacked piezoelectric actuators. J Sound Vib 292(1–2):203–220. doi:10.1016/j.jsv.2005.07.040, http://www.sciencedirect.com/science/article/pii/S0022460X050 05171
75. NASA Dryden Flight Research Center (NASA-DFRC) (2001) The Aerostructures Test Wing (ATW)— after intentional failure. Image ID: EC01-0124-1
76. NASA Dryden Flight Research Center (NASA-DFRC) (2001) The Aerostructures Test Wing (ATW)— before failure. Image ID: EC01-0086-4
77. NASA Dryden Flight Research Center (NASA-DFRC) (2001) The Aerostructures Test Wing (ATW) experiment (description). Online, http://nix.larc.nasa.gov/info;jsessionid=6f0l4hj7bt39u?id=EC01-0086-4\&orgid=7
78. NASA Glenn Research Center (NASA-GRC) (2008) Shape Memory Alloy (SMA) Demonstration Hardware. Image ID: C-2008-02698
79. NASA Glenn Research Center (NASA-GRC) (2008) Shape Memory Alloy (SMA) Demonstration Hardware. Image ID: C-2008-02707
80. NASA Langley Research Center (NASA-LaRC) (1996) High Displacement Actuator (HDA). Image ID: EL-1996-00133
81. NASA Langley Research Center (NASA-LaRC) (2000) F-15 model in the 16 foot transonic tunnel. Image ID: EL-2000-00147
82. NASA Marshall Space Flight Center (NASA-MSFC) (2002) Comparison of magnetorheological fluids on earth and in space. Image ID: MSFC-0700441
83. Ngatu GT, Wereley NM, Karli JO, Bell RC (2008) Dimorphic magnetorheological fluids: exploiting partial substitution of microspheres by nanowires. Smart Mater Struct 17(4):045,022, http://stacks.iop.org/0964-1726/17/i=4/a=045022
84. Palakodeti R, Kessler M (2006) Influence of frequency and prestrain on the mechanical efficiency of dielectric electroactive polymer actuators. Mater Lett 60(29–30):3437–3440. doi:10.1016/j.matlet.2006.03.053, http://www.sciencedirect.com/science/article/B6TX9-4JN2J11-2/2/bb86365e0ad88fd27e7dad13bd4d5ac0
85. Park JS, Kim JH, Moon SH (2004) Vibration of thermally post-buckled composite plates embedded with shape memory alloy fibers. Compos Struct 63(2):179–188, doi:10.1016/S0263-8223(03)00146-6, http://www.sciencedirect.com/science/article/B6TWP-48Y6PS8-6/2/d70ea3b2717f54027d999c7fe92da11f
86. Phillips DJ, Hyland DC, Collins CG (2002) Real-time seismic damping and frequency control of steel structures using nitinol wire. In: Proceedings of SPIE 2002, vol 4696, pp 176–185

87. Piefort V (2001) Finite element modelling of piezoelectric structures. PhD thesis, Université Libre de Bruxelles
88. Piezosystem-Jena (2007) Piezoline theory. Available: http://www.piezojena.com/files.php4?dl_mg_id=229\&file=dl_mg_1195142143.pdf\&SID=125nfb5prkpt35d2k9cops3021
89. Pilgrim SM (2001) Electrostrictive ceramics for sonar projectors. In: Buschow KHJ, Cahn RW, Flemings MC, Ilschner B, Kramer EJ, Mahajan S, Veyssicre P (eds) Encyclopedia of materials: science and technology, Elsevier, Oxford, pp 2738–2743. doi:10.1016/B0-08-043152-6/00488-5, http://www.sciencedirect.com/science/article/B7NKS-4KF1VT9-MR/2/9a3a6454bb6c54bb64719b3036d2789b
90. Pradhan S (2005) Vibration suppression of FGM shells using embedded magnetostrictive layers. Int J Solids Struct 42(9–10):2465–2488, doi:10.1016/j.ijsolstr.2004.09.049, http://www.sciencedirect.com/science/article/B6VJS-4F6SSGN-1/2/b6f9e2e6ffc65bfc0c4af5083e37df0b
91. Preumont A (2002) Vibration control of active structures, 2nd edn. Kluwer Academic Publishers, Dordrecht
92. Preumont A, Seto K (2008) Active control of structures, 3rd edn. Wiley, Chichester
93. Rajoria H, Jalili N (2005) Passive vibration damping enhancement using carbon nanotube-epoxy reinforced composites. Compos Sci Technol 65(14):2079–2093. doi:10.1016/j.compscitech.2005.05.015, http://www.sciencedirect.com/science/article/B6TWT-4GHBPN0-5/2/a67d954050aac7829a56e3e4302c8ef6
94. Ren TL, Zhao HJ, Liu LT, Li ZJ (2003) Piezoelectric and ferroelectric films for microelectronic applications. Mater Sci Eng B 99(1–3):159–163. doi:10.1016/S0921-5107(02)00466-X, http://www.sciencedirect.com/science/article/B6TXF-47P92FB-4/2/4f139e078631af2acf841b7db5d37316, Advanced electronic-ceramic materials. Proceedings of the 8th IUMRS international conference on electronic materials (IUMRS-ICEM2002), Symposium N
95. Richter H, Misawa EA, Lucca DA, Lu H (2001) Modeling nonlinear behavior in a piezoelectric actuator. Precis Eng 25(2):128–137. doi:10.1016/S0141-6359(00)00067-2, http://www.sciencedirect.com/science/article/pii/S0141635900000672
96. Rossing TD, Moore RF, Wheeler PA (2001) The science of sound. 3rd edn. Addison Wesley, San Francisco
97. Schlacher K, Kugi A, Irschik H (1998) $\mathscr{H}_\infty$-control of random structural vibrations with piezoelectric actuators. Comput Struct 67(1–3):137–145. doi:10.1016/S0045-7949(97)00165-X, http://www.sciencedirect.com/science/article/B6V28-3VKTNM7-J/2/faecf09ede8e0d56452351d4d30bc45b
98. Shin HC, Choi SB (2001) Position control of a two-link flexible manipulator featuring piezoelectric actuators and sensors. Mechatronics 11(6):707–729. doi:10.1016/S0957-4158(00)00045-3, http://www.sciencedirect.com/science/article/B6V43-43MMSYG-8/2/868a8129a5636d164e6aa1a89358b8fb
99. Sitnikova E, Pavlovskaia E, Wiercigroch M, Savi MA (2010) Vibration reduction of the impact system by an SMA restraint: numerical studies. Int J Non Linear Mech 45(9):837–849. doi:10.1016/j.ijnonlinmec.2009.11.013, http://www.sciencedirect.com/science/article/B6TJ2-4Y4PVRH-1/2/6c55c60479b498920a5272d281d5fd5d, dynamics, control and design of nonlinear systems with smart structures
100. Sodano HA, Inman DJ (2007) Non-contact vibration control system employing an active eddy current damper. J Sound Vib 305(4–5):596–613. doi:10.1016/j.jsv.2007.04.050 http://www.sciencedirect.com/science/article/B6WM3-4P2J38T-3/2/a75ecce7ed7841e00499a50d077bd23c
101. Song G, Ma N, Li HN (2006) Applications of shape memory alloys in civil structures. Eng Struct 28(9):1266–1274. doi:10.1016/j.engstruct.2005.12.010, http://www.sciencedirect.com/science/article/B6V2Y-4JRM0BH-1/2/ccac39dd197a6414511170 34df623bd1
102. Song G, Sethi V, Li HN (2006) Vibration control of civil structures using piezoceramic smart materials: a review. Eng Struct 28(11):1513–1524,

doi:10.1016/j.engstruct.2006.02.002, http://www.sciencedirect.com/science/article/B6V2Y-4JKRTRW-3/2/73299aa5fc196cb9802cbc961b896402
103. Spelta C, Previdi F, Savaresi SM, Fraternale G, Gaudiano N (2009) Control of magnetorheological dampers for vibration reduction in a washing machine. Mechatronics 19(3):410–421. doi:10.1016/j.mechatronics.2008.09.006, http://www.sciencedirect.com/science/article/B6V43-4TT1G22-1/2/3d8e5bd1cc63e7181272ef848f15508c
104. Stangroom JE (1983) Electrorheological fluids. Phys Technol 14(6):290. http://stacks.iop.org/0305-4624/14/i=6/a=305
105. Stanway R (2004) Smart fluids: current and future developments. Mater Sci Technol 20(8):931–939
106. Stöppler G, Douglas S (2008) Adaptronic gantry machine tool with piezoelectric actuator for active error compensation of structural oscillations at the tool centre point. Mechatronics 18(8):426–433, doi:10.1016/j.mechatronics.2008.03.002, http://www.sciencedirect.com/science/article/B6V43-4SC5PJV-2/2/ca3951fdc7496b096233f1bd02e0898a
107. Su YX, Duan BY, Wei Q, Nan RD, Peng B (2002) The wind-induced vibration control of feed supporting system for large spherical radio telescope using electrorheological damper. Mechatronics 13(2):95–110. doi:10.1016/S0957-4158(01)00042-3, http://www.sciencedirect.com/science/article/B6V43-46WPHMS-2/2/eca7cd44909e99a1f8c6ad76a4fd4f19
108. Suleman A, Costa AP (2004) Adaptive control of an aeroelastic flight vehicle using piezoelectric actuators. Comput Struct 82(17–19):1303–1314. doi:10.1016/j.compstruc.2004.03.027, http://www.sciencedirect.com/science/article/B6V28-4CPD4P5-1/2/5a9c6f2a79e0f4e978f43d2b6ed45b93, computational mechanics in Portugal
109. Suleman A, Burns S, Waechter D (2004) Design and modeling of an electrostrictive inchworm actuator. Mechatronics 14(5):567–586. doi:10.1016/j.mechatronics.2003.10.007, http://www.sciencedirect.com/science/article/B6V43-49YD001-1/2/9b6a81729c9e0f3c7f59ce4bafbe5c2a
110. Sung KG, Han YM, Cho JW, Choi SB (2008) Vibration control of vehicle ER suspension system using fuzzy moving sliding mode controller. J Sound Vib 311(3–5):1004–1019. doi:10.1016/j.jsv.2007.09.049, http://www.sciencedirect.com/science/article/B6WM3-4R2H1TN-4/2/b3a297765c3ac7767b2d64fda7a6a3d7
111. Tabak F, Disseldorp E, Wortel G, Katan A, Hesselberth M, Oosterkamp T, Frenken J, van Spengen W (2010) MEMS-based fast scanning probe microscopes. Ultramicroscopy 110(6):599–604. doi:10.1016/j.ultramic.2010.02.018, http://www.sciencedirect.com/science/article/B6TW1-4YJCKXY-1/2/4f5b9ba5875b8066d7cb20174f05ad61, 11th International scanning probe microscopy conference
112. Takács G, Rohal'-Ilkiv B (2009) Implementation of the Newton-Raphson MPC algorithm in active vibration control applications. In: Mace BR, Ferguson NS, Rustighi E (eds) Proceedings of the 3rd international conference on noise and vibration: emerging methods, Oxford
113. Takács G, Rohal'-Ilkiv B (2009) MPC with guaranteed stability and constraint feasibility on flexible vibrating active structures: a comparative study. In: Hu H (ed) Proceedings of the 11th IASTED international conference on control and applications, Cambridge
114. Takács G, Rohal'-Ilkiv B (2009) Newton-Raphson based efficient model predictive control applied on active vibrating structures. In: Proceedings of the European control control conference, Budapest
115. Takács G, Rohal'-Ilkiv B (2009) Newton-Raphson MPC controlled active vibration attenuation. In: Hangos KM (ed) Proceedings of the 28th IASTED international conference on modeling, identification and control, Innsbruck
116. TRS Technologies (2010) Electrostrictive materials. State College. Online, http://www.trstechnologies.com/Materials/electrostrictive_materials.php
117. Tzou H, Chai W (2007) Design and testing of a hybrid polymeric electrostrictive/piezoelectric beam with bang-bang control. Mech Syst Sig Process 21(1):417–429. doi:10.1016/j.ymssp.2005.10.008, http://www.sciencedirect.com/science/article/B6WN1-4HR75KY-1/2/73701e5908a2ea598fa7bec1ce093563

118. Van den Broeck L, Diehl M, Swevers J (2009) Time optimal MPC for mechatronic applications. In: Proceedings of the 48th IEEE conference on decision and control, Shanghai, pp 8040–8045
119. Van den Broeck L, Swevers J, Diehl M (2009) Performant design of an input shaping prefilter via embedded optimization. In: Proceedings of the 2009 American control conference, St-Louis, pp 166–171
120. Vereda F, de Vicente J, Hidalgo-Álvarez R (2009) Physical properties of elongated magnetic particles: Magnetization and friction coefficient anisotropies. ChemPhysChem 10:1165–1179
121. Wahed AKE, Sproston JL, Schleyer GK (2002) Electrorheological and magnetorheological fluids in blast resistant design applications. Mater Des 23(4):391–404. doi: 10.1016/S0261-3069(02)00003-1, http://www.sciencedirect.com/science/article/B6TX5-450HD50-1/2/0da443f054d99983150525d47bf17aeb
122. Wang H, Zheng H, Li Y, Lu S (2008) Mechanical properties of magnetorheological fluids under squeeze-shear mode. In: Society of photo-optical instrumentation engineers (SPIE) conference series, presented at the Society of Photo-optical Instrumentation Engineers (SPIE) conference, vol 7130. doi:10.1117/12.819634
123. Wang M, Fei R (1999) Chatter suppression based on nonlinear vibration characteristic of electrorheological fluids. Int J Mach Tools Manuf 39(12):1925–1934. doi:10.1016/S0890-6955(99)00039-5, http://www.sciencedirect.com/science/article/B6V4B-3X7N8GJ-7/2/6cc38d51af69b4fbb0aa1135681b5356
124. Wei JJ, Qiu ZC, Han JD, Wang YC (2010) Experimental comparison research on active vibration control for flexible piezoelectric manipulator using fuzzy controller. J Intell Rob Syst 59:31–56, doi:10.1007/s10846-009-9390-2, http://dx.DOI.org/10.1007/s10846-009-9390-2
125. Williams E, Rigby S, Sproston J, Stanway R (1993) Electrorheological fluids applied to an automotive engine mount. J Non-Newtonian Fluid Mech 47:221–238. doi: 10.1016/0377-0257(93)80052-D, http://www.sciencedirect.com/science/article/B6TGV-44V49DV-75/2/a6f4db8ffcb810f6167c845a984dd93f
126. Williams K, Chiu G, Bernhard R (2002) Adaptive-passive absorbers using shape-memory alloys. J Sound Vib 249(5):835–848. doi:10.1006/jsvi.2000.3496, http://www.sciencedirect.com/science/article/B6WM3-4576DS3-2N/2/63e7f46640d919db867f8b1e391f4c4c
127. Wills AG, Bates D, Fleming AJ, Ninness B, Moheimani SOR (2008) Model predictive control applied to constraint handling in active noise and vibration control. IEEE Trans Control Syst Technol 16(1):3–12
128. Yan G, Sun B, Lü Y (2007) Semi-active model predictive control for 3rd generation benchmark problem using smart dampers. Earthq Eng Eng Vib 6:307–315. doi:10.1007/s11803-007-0645-2, http://dx.DOI.org/10.1007/s11803-007-0645-2
129. Yeh TJ, Ruo-Feng H, Shin-Wen L (2008) An integrated physical model that characterizes creep and hysteresis in piezoelectric actuators. Simul Modell Pract Theory 16(1):93–110. doi:10.1016/j.simpat.2007.11.005, http://www.sciencedirect.com/science/article/pii/S1569190X07001396
130. Yongsheng R, Shuangshuang S (2007) Large amplitude flexural vibration of the orthotropic composite plate embedded with shape memory alloy fibers. Chin J Aeronaut 20(5):415–424. doi:10.1016/S1000-9361(07)60063-6, http://www.sciencedirect.com/science/article/B8H0X-4R5R8KJ-5/2/dfb4a7094008193f73ce3269cb319dbe
131. Yuse K, Guyomar D, Kanda M, Seveyrat L, Guiffard B (2010) Development of large-strain and low-powered electro-active polymers (EAPs) using conductive fillers. Sens Actuators A. In Press, Accepted Manuscript. doi:10.1016/j.sna.2010.08.008, http://www.sciencedirect.com/science/article/B6THG-50RVNJK-5/2/4002a5f80bb3323c2a1a5af618b089ca
132. Zhang X, Lu J, Shen Y (2003) Active noise control of flexible linkage mechanism with piezoelectric actuators. Comput Struct 81(20):2045–2051. doi:10.1016/S0045-7949(03)00230-X, http://www.sciencedirect.com/science/article/B6V28-49036KY-2/2/418991ffedba1e4e78d0f90c263b465e

133. Zhou C, Liu X, Li W, Yuan C, Chen G (2010) Structure and electrical properties of Bi_0.5 (Na, K)$_0$.5 TiO_3-$BiGao_3$ lead-free piezoelectric ceramics. Curr Appl Phys 10(1):93–98. doi:10.1016/j.cap.2009.05.004, http://www.sciencedirect.com/science/article/B6W7T-4WBC1T8-1/2/8caea987dd9c442dea9061d54474df0e
134. Zhu C (2005) A disk-type magneto-rheological fluid damper for rotor system vibration control. J Sound Vib 283(3-5):1051–1069. doi:10.1016/j.jsv.2004.06.031, http://www.sciencedirect.com/science/article/B6WM3-4F4H9R2-1/2/48abebbf8d1230fcd80eee7d19fe52fa